MCB
Journals.ASM.org

TAK1 Is Essential for Osteoclast Differentiation and Is an Important Modulator of Cell Death by Apoptosis and Necroptosis

Betty Lamothe,[a] YunJu Lai,[a] Min Xie,[b] Michael D. Schneider,[c] Bryant G. Darnay[a]

Department of Experimental Therapeutics, The University of Texas M. D. Anderson Cancer Center, Houston, Texas, USA[a]; Department of Internal Medicine, University of Texas Southwestern Medical Center, Dallas, Texas, USA[b]; Faculty of Medicine, National Heart and Lung Institute, Imperial College London, London, United Kingdom[c]

Transforming growth factor β (TGF-β)-activated kinase 1 (TAK1), a mitogen-activated protein 3 (MAP3) kinase, plays an essential role in inflammation by activating the IκB kinase (IKK)/nuclear factor κB (NF-κB) and stress kinase (p38 and c-Jun N-terminal kinase [JNK]) pathways in response to many stimuli. The tumor necrosis factor (TNF) superfamily member receptor activator of NF-κB ligand (RANKL) regulates osteoclastogenesis through its receptor, RANK, and the signaling adaptor TRAF6. Because TAK1 activation is mediated through TRAF6 in the interleukin 1 receptor (IL-1R) and toll-like receptor (TLR) pathways, we sought to investigate the consequence of TAK1 deletion in RANKL-mediated osteoclastogenesis. We generated macrophage colony-stimulating factor (M-CSF)-derived monocytes from the bone marrow of mice with TAK1 deletion in the myeloid lineage. Unexpectedly, TAK1-deficient monocytes in culture died rapidly but could be rescued by retroviral expression of TAK1, inhibition of receptor-interacting protein 1 (RIP1) kinase activity with necrostatin-1, or simultaneous genetic deletion of TNF receptor 1 (TNFR1). Further investigation using TAK1-deficient mouse embryonic fibroblasts revealed that TNF-α-induced cell death was abrogated by the simultaneous inhibition of caspases and knockdown of RIP3, suggesting that TAK1 is an important modulator of both apoptosis and necroptosis. Moreover, TAK1-deficient monocytes rescued from programmed cell death did not form mature osteoclasts in response to RANKL, indicating that TAK1 is indispensable to RANKL-induced osteoclastogenesis. To our knowledge, we are the first to report that mice in which TAK1 has been conditionally deleted in osteoclasts develop osteopetrosis.

Receptor activator of nuclear factor κB (NF-κB) (RANK) ligand (RANKL) and RANK are important to osteoclast formation, since mice lacking either of these genes exhibited severe osteopetrosis due to a complete failure to form osteoclasts (1, 2). Like most members of the tumor necrosis factor (TNF) receptor (TNFR) superfamily, RANK engages TNF receptor-associated factors (TRAFs) to activate several kinase cascades including IκB kinase (IKK) and mitogen-activated protein kinases (MAPKs) (e.g., p38 and c-Jun N-terminal kinase [JNK]), to induce transcription factors, such as NF-κB Fos, and nuclear factor of activated T cells 1 (NFATc1) (3). This induction in turn leads to osteoclast differentiation and the expression of osteoclastic genes (4).

Previous studies have shown that TRAF6-deficient mice develop severe osteopetrosis (5, 6) and that osteoclast differentiation *ex vivo* is completely abolished (7, 8), indicating that TRAF6 is the major adaptor molecule of RANK signaling during osteoclastogenesis. Other studies found that compared with their control littermates, mice with IKKβ deleted in the myeloid lineage had higher bone mass, fewer osteoclasts, and impaired osteoclast survival that could be rescued on a TNFR1-null background without preventing osteopetrosis (9, 10).

Transforming growth factor β (TGF-β)-activated kinase 1 (TAK1), a member of the MAPK kinase kinase (MAP3K) family, is essential to activating the IKK/NF-κB pathways and the stress kinase (i.e., JNK and p38 MAPK) pathways in response to various inflammatory molecules and cytokines (11, 12). Through its really interesting new gene (RING)-dependent ubiquitin ligase activity, TRAF6 facilitates the synthesis of nondegradative Lys-63-linked polyubiquitin chains to recruit and activate TAK1; this recruitment in turn activates IKK to initiate the NF-κB pathway and activates MKK6 and MKK7 to induce the JNK and p38 MAPK pathways, respectively (13–16).

A dominant negative form of TAK1 that inhibits RANK signaling (17–19) and the blocking of the interaction between TAK1 and TAK1 binding protein 2 (TAB2) (20) have been used to investigate the role of TAK1 in RANK signaling. Although these studies provided evidence of the function of TAK1 in RANK signaling, their findings are not physiologically relevant to the investigation of the effects of TAK1 deficiency in RANKL-induced osteoclastogenesis and thus cannot reveal any possible compensatory mechanisms. To date, the functional consequences TAK1 loss has for osteoclastogenesis *in vitro* and *in vivo* have not been evaluated. Since TAK1 is the key intermediate bridging TRAF6 to IKKβ, both of which are critical regulators of RANKL-mediated osteoclastogenesis (7–10), the function of TAK1 in this process will add to our understanding of osteoclast biology.

In the present study, to determine the consequences of TAK1 deficiency on osteoclastogenesis *in vitro*, we crossed TAK1-floxed mice with lysozyme M-Cre recombinase (LysM-Cre) knock-in mice to delete TAK1 in osteoclast precursors. To determine these consequences *in vivo*, we crossed TAK1-floxed mice with cathepsin K-Cre (Ctsk-Cre) knock-in mice to delete TAK1 in osteoclasts. Our findings indicate that loss of TAK1 in osteoclast precursors affects their homeostasis and their responses to RANKL-induced signaling events *in vitro* and that loss of TAK1 in osteoclasts affects bone remodeling *in vivo*.

Received 5 September 2012 **Returned for modification** 4 October 2012
Accepted 13 November 2012
Published ahead of print 19 November 2012
Address correspondence to Bryant G. Darnay, bdarnay@mdanderson.org, or Betty Lamothe, blamothe@mdanderson.org.

doi:10.1128/MCB.01225-12

MATERIALS AND METHODS

Generation of conditional knockout of TAK1 in the osteoclast lineage. LysM-Cre knock-in mice (21) were purchased from The Jackson Laboratory (Bar Harbor, ME). Ctsk-Cre knock-in mice were provided by Shigeaki Kato (University of Tokyo, Tokyo, Japan) (22).

Mice carrying the floxed allele of TAK1 ($TAK1^{F/F}$) and the null allele of TAK1 ($TAK1^{+/-}$) have been described previously (23). $TAK1^{F/F}$-$LysM^{+/+}$ mice were crossed with $TAK1^{+/-}$-$LysM^{cre/cre}$ mice to generate offspring lacking TAK1 in the myeloid lineage ($TAK1^{\Delta M}$) or heterozygote mice ($TAK1^{F/+}$). $TAK1^{F/+}$-$Ctsk^{+/+}$ mice were crossed with $TAK1^{+/-}$-$Ctsk^{cre/cre}$ mice to produce offspring lacking TAK1 in differentiating osteoclasts ($TAK1^{\Delta OC}$), heterozygote mice ($TAK1^{F/+}$), or wild-type (WT) mice ($TAK1^{+/+}$). Mice were genotyped by subjecting tissue from ear clips to standard PCR. TNFR1-null $TAK1^{\Delta M}$ or $TAK1^{\Delta OC}$ mice were generated by crossing $TAK1^{\Delta M}$ or $TAK1^{\Delta OC}$ mice with TNFR1-deficient mice obtained from The Jackson Laboratory.

All mice had been backcrossed to C57BL/6 mice 6 to 9 generations at the time of the experiments. Mice were housed in a pathogen-free animal facility. All mouse experiments were approved by The University of Texas M. D. Anderson Cancer Center's Institutional Animal Care and Use Committee. Mice were cared for in accordance with guidelines set forth by the American Association for Accreditation of Laboratory Animal Care and the U.S. Public Health Service Policy on Humane Care and Use of Laboratory Animals.

Cell lines, retroviral vectors, antibodies, and reagents. The retroviral packaging cell line GP2-293 was purchased from Clontech (Palo Alto, CA) and cultured as described previously (7, 14). HEK293T cells were a gift from Xin Lin (Department of Molecular and Cellular Oncology, M. D. Anderson Cancer Center). TAK1-knockout (KO) mouse embryonic fibroblasts (MEFs) were generated by transient transfection of the Cre recombinase in immortalized $TAK1^{F/F}$ MEFs, and loss of TAK1 protein expression was verified using immunoblot analysis. The L929-GFP and L929-TAK1-C100 cell lines and the retroviral vectors pMX and pMX-TAK1 have been described previously (20). The pLKO.1-based receptor-interacting protein 3 (RIP3) short hairpin RNA (shRNA) (TRCN0000022535) was obtained from Open Biosystems (Lafayette, CO), and the luciferase shRNA (TRCN0000072244) was used as a negative control. Biocoated Osteologic discs were purchased from BD Biosciences (San Jose, CA). Antibodies against phospho-IκBα, phospho-p38, p38, phospho-c-Jun, and caspase-3 were purchased from Cell Signaling Technology (Beverly, MA). Antibodies against JNK, c-Jun, TAK1, IκBα, and Fas-associated death domain (FADD) were purchased from Santa Cruz Biotechnology, Inc. (Santa Cruz, CA). β-Actin was purchased from Cytoskeleton (Denver, CO), RIP3 from Proscience Inc. (Poway, CA), caspase-8 from Alexis Biochemicals (Lausen, Switzerland), RIP1 from BD Transduction Laboratories (Lexington, KY), goat anti-rabbit immunoglobulin G-conjugated horseradish peroxidase from Bio-Rad (Hercules, CA), and goat anti-mouse immunoglobulin G-conjugated horseradish peroxidase from BD Biosciences (San Diego, CA). A monoclonal anti-FLAG antibody and the tartrate-resistant acid phosphatase (TRAP) staining kit were purchased from Sigma (St. Louis, MO). Recombinant macrophage colony-stimulating factor (M-CSF) and the caspase inhibitors zVAD-fmk and zIETD-fmk were purchased from R&D Systems (Minneapolis, MN). Necrostatin-1 (Nec-1) was purchased from Enzo Life Biosciences (Farmingdale, NY). TNF-α was purchased from PreproTech EC Ltd. (Rocky Hill, NJ). L929-M-CSF conditioned medium (LCM), recombinant mouse RANKL, and glutathione *S*-transferase–c-Jun were purified as described previously (7, 14, 24).

Culture and treatment of primary mouse monocytes and differentiation of osteoclasts. Bone marrow (BM) cells were isolated from the femurs of 6- to 10-week-old control or conditional knockout mice. Collagenase was used to extract splenic cells from 1- to 6-day-old control or conditional knockout mice. Isolated cells were cultured for 24 h in α-minimal essential medium supplemented with 10% fetal bovine serum. The nonadherent BM-derived monocytes (BMMs) or spleen-derived monocytes were collected and cultured with 5% LCM or recombinant M-CSF as described previously (7, 14) for the indicated times. Phase-contrast and fluorescent images of live cells and phase-contrast images of fixed cells stained with crystal violet or TRAP were taken using a Nikon Eclipse TE2000-U microscope.

For the assessment of the signaling events induced by RANKL, BMMs or differentiated osteoclasts were washed twice with phosphate-buffered saline, incubated for 3 h in serum-free medium without M-CSF, and stimulated with RANKL. Osteoclast differentiation and TRAP staining were performed as described previously (7, 14). To determine whether TAK1 rescued BMMs from cell death and osteoclast differentiation, BM cells from $TAK1^{\Delta M}$ mice were incubated in the presence of retroviral supernatant for 24 h; nonadherent cells were replated in the presence of M-CSF and the retroviral supernatant for an additional 12 h. The cells were then incubated with M-CSF in fresh medium with or without RANKL (100 ng/ml). The medium was changed every 2 days until the appearance of osteoclasts, which were then fixed and stained for TRAP. For the osteoclast pit formation assay, osteoclasts differentiated on calcium phosphate-coated Osteologic discs were removed with bleach, and the resorbed areas were quantified using the MetaVue image software program (version 6.1; Downingtown, PA). The Alpha Innotech Imaging system (Santa Clara, CA) was used to measure the area occupied by the osteoclasts in 10 different fields. Nuclei per osteoclast were counted manually in 10 different fields.

Bone histomorphometry. Soft tissue was removed from the tibias and femurs of mice, and the bones were fixed in formalin for 24 h at 4°C and then stored in 70% ethanol. Histomorphometry analysis of TRAP-stained bones was performed by the Bone Histomorphometry Core Laboratory at M. D. Anderson Cancer Center. All bone-specific parameters were measured and expressed in units following the guidelines established by the American Society for Bone and Mineral Research histomorphometry nomenclature committee (25).

Immunoblotting, immunoprecipitation, and kinase assays. Cell lysate preparation, immunoblotting, immunoprecipitation, and *in vitro* kinase assays were performed as described previously (7, 14, 26).

Viability assay. BMMs were plated either at low density (2.5×10^4 cells) or at high density (5.0×10^4 cells) in triplicate in 96-well plates in the presence of 5% LCM or recombinant M-CSF. MEFs and L929 cells (2×10^4) were plated in 96-well plates. The XTT assay (Roche Diagnostic Corp., Germany) was used to assess cell viability. Viable cells were counted at the indicated times by adding 50 μl of XTT mix prepared according to the manufacturer's instructions to 200 μl of culture medium in each well and then incubating the cells in the dark at 37°C for 4 h. The absorbance at 570 nm was measured. Cell viability was also assessed by staining the cells with crystal violet. The stain was solubilized with Sorensen's buffer, and the absorbance at 595 nm was measured. In addition, cell viability was assessed using the CellTiter-Glo Luminescent Cell Viability assay (Promega Corporation, Madison, WI) according to the manufacturer's protocol.

PI and Hoechst 33342 staining. BMMs and MEFs were incubated with 4 μg/ml of propidium iodide (PI) or 4 μg/ml of PI plus 1 μg/ml of Hoechst dye, respectively, diluted in 0.2% bovine serum albumin–phosphate-buffered saline for 20 min at 37°C. For quantification of PI-positive cells in the BMMs, photographs of 9 individual fields were taken using a fluorescence microscope. PI-positive and total cells were manually counted, and the percentages of PI-positive cells were recorded. Cells with chromatin condensation were visualized by Hoechst staining and counted as apoptotic.

Data analysis. Where indicated, values are expressed as means ± standard deviations. An unpaired two-tailed Student *t* test was used to assess differences between experimental groups. *P* values of <0.05 were considered statistically significant.

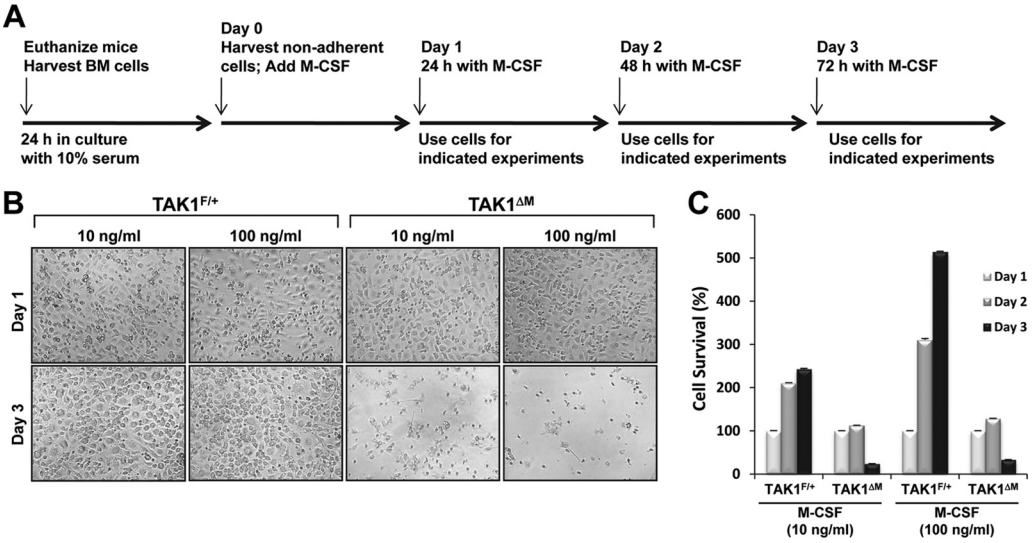

FIG 1 TAK1-deficient BMMs undergo spontaneous cell death in culture. (A) Timeline of the different experimental procedures. (B and C) High-dose M-CSF does not rescue TAK1$^{\Delta M}$ monocytes from cell death. BM cells were treated with M-CSF (10 or 100 ng/ml), and on the morning of day 1, the cells were lifted from the plate, counted, and replated in the presence of M-CSF (10 or 100 ng/ml). Representative phase-contrast images were taken the evening of day 1 and the evening of day 3 (B). Cell survival was measured by using the XTT assay (C).

RESULTS

Survival defect of TAK1-deficient monocytes. Primary mouse BMMs can be generated *in vitro* by growing whole BM in the presence of M-CSF over 3 days. The addition of RANKL to these cultures initiates a differentiation program that evokes the terminal differentiation of monocytes into mature, multinucleated osteoclasts. To obtain a source of osteoclast precursors to study the ways in which loss of TAK1 affects RANKL-induced osteoclastogenesis, we used the LysM-Cre (21) model to generate M-CSF-derived monocytes from BM precursors of mice conditionally deficient in TAK1 in the myeloid lineage. The mice were generated by crossing TAK1$^{F/F}$-LysM$^{+/+}$ mice with TAK1$^{+/-}$-LysM$^{Cre/Cre}$ mice to produce TAK1$^{F/+}$-LysM$^{Cre/+}$ (TAK1$^{F/+}$) or TAK1$^{F/-}$-LysM$^{Cre/+}$ (TAK1$^{\Delta M}$, deleted in monocytes) littermates. The methodology used to treat the BMMs is illustrated in Fig. 1A. Microscopic analysis did not reveal any gross morphological abnormalities in the appearance of M-CSF-dependent BMMs isolated from TAK1$^{F/+}$ or TAK1$^{\Delta M}$ mice on day 1 (Fig. 1B). Unlike the TAK1$^{F/+}$ monocytes, the TAK1$^{\Delta M}$ monocytes died between 48 and 72 h in culture with M-CSF (Fig. 1B and C, day 3). Moreover, phase-contrast photographs and survival assessment using the XTT assay indicated that even a high concentration of M-CSF (100 ng/ml) did not rescue TAK1$^{\Delta M}$ monocytes from death (Fig. 1B and C), which is consistent with a previous study showing that TAK1-deficient BMMs died after 3 days in culture (27). This observation is in contrast to those of previous reports, in which monocytes deficient in IKKβ, an immediate downstream signaling effector of TAK1, survived in the presence of M-CSF (9, 10).

We next sought to determine whether TAK1$^{\Delta M}$ monocytes provided with exogenous TAK1 are able to survive in the presence of M-CSF. We used a retroviral expression system (7, 14) that expresses green fluorescent protein (GFP) to introduce TAK1 into the TAK1$^{\Delta M}$ monocytes during the first 2 days of culture. Fluorescence microscopy analysis on day 1 revealed similar numbers of GFP-positive TAK1$^{\Delta M}$ cells infected with TAK1 (pMX-TAK1) and TAK1$^{\Delta M}$ cells infected with empty vector (pMX) (Fig. 2A). The cellular confluence was also similar, as indicated by crystal violet staining (Fig. 2A). The expression of exogenous TAK1 was confirmed by immunoblotting with an anti-TAK1 antibody (Fig. 2B, left panel). TAK1$^{\Delta M}$ monocytes infected with the empty vector died (Fig. 2C, top panel), whereas exogenous expression of TAK1, but not a kinase-dead TAK1 (data not shown), rescued the ability of TAK1$^{\Delta M}$ monocytes to survive in the presence of M-CSF (Fig. 2C, top panel). In addition, RANKL stimulated JNK activation in the TAK1$^{\Delta M}$ monocytes infected with TAK1 but not the empty vector (Fig. 2B, right panel). In a manner similar to that in TAK1$^{F/+}$ BMMs (Fig. 2C, bottom panel), expression of TAK1 in TAK1-deficient monocytes enabled the development of large, multinucleated TRAP^{+} osteoclasts following stimulation with M-CSF and RANKL. Taken together, these results provide evidence that the absence of TAK1 is primarily responsible for the survival defect of TAK1$^{\Delta M}$ monocytes.

Deletion of TNFR1 rescues TAK1-deficient BMM survival. Previous reports have shown that primary TAK1-deficient cells generated from conditional knockout mice have shorter survival times *ex vivo* and are typically more sensitive to apoptotic stimuli such as TNF-α (11, 12, 28–31). Our cell viability assay revealed that TAK1$^{\Delta M}$ monocytes were sensitive to TNF-α-mediated cell death (Fig. 3A). Because macrophages express very low levels of TNF-α in response to M-CSF in tissue culture (32) and TNFR1 initiates apoptosis or necroptosis, we next sought to determine whether TNFR1 plays a role in the death of TAK1$^{\Delta M}$ monocytes. We crossed TAK1-floxed LysM-Cre mice with mice containing global deletion of TNFR1 (TNFR1$^{-/-}$) to obtain monocytes lacking both TAK1 and TNFR1 and found that unlike TAK1$^{\Delta M}$ monocytes, TAK1$^{\Delta M}$-TNFR1$^{-/-}$ monocytes survived (Fig. 3B and C). These results indicate that TAK1-deficient monocyte death is TNFR1 dependent.

TAK1 is essential to RANKL-induced osteoclast formation. The survival of TAK1$^{\Delta M}$-TNFR1$^{-/-}$ BMMs in the presence of

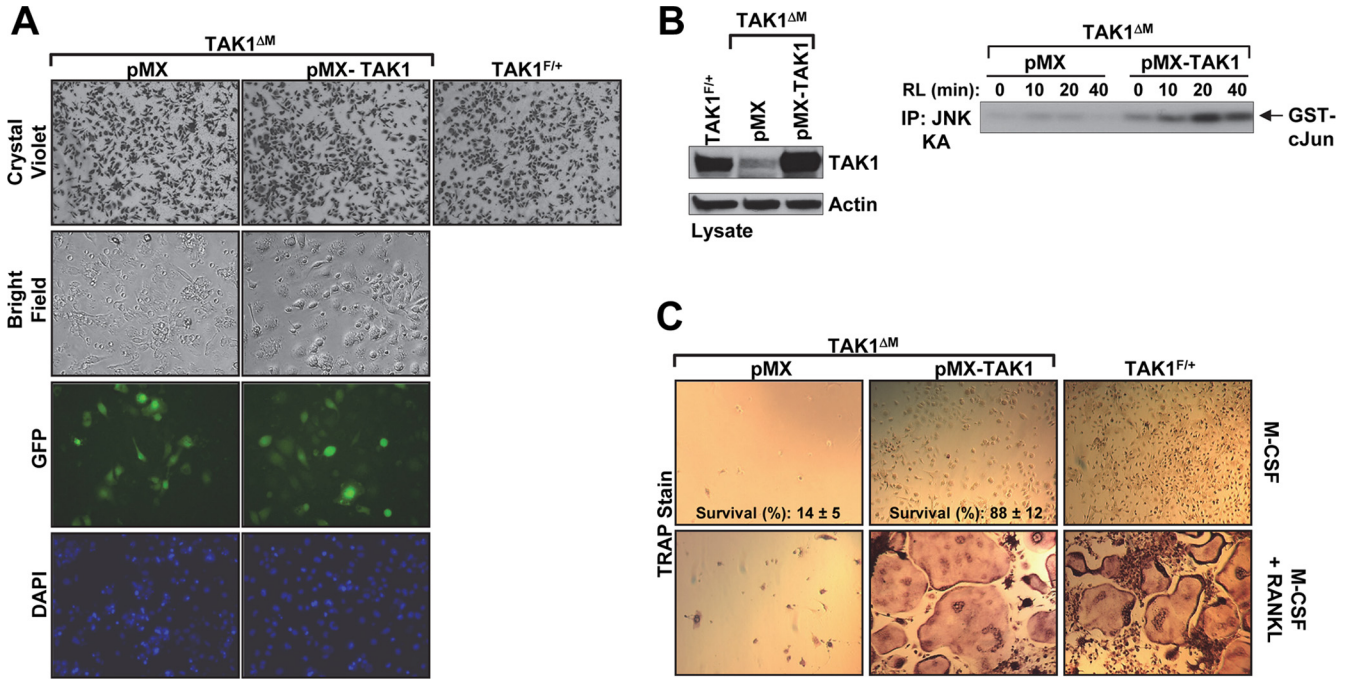

FIG 2 Retroviral delivery of TAK1 rescues survival of TAK1-deficient monocytes and osteoclast differentiation. (A to C) TAK1$^{\Delta M}$ BMMs were infected with retroviral supernatant expressing empty vector (pMX) or TAK1 (pMX-TAK1). After 2 days, phase-contrast and fluorescence microscopy images of the infected TAK1$^{\Delta M}$ BMMs and control TAK1$^{F/+}$ BMMs were obtained. The cells were then fixed and stained with crystal violet (A). The cells were lysed and immunoblotted as indicated (B, left panel). Infected TAK1$^{\Delta M}$ BMMs were stimulated with RANKL (RL,100 ng/ml) as indicated, and JNK activity was measured using an *in vitro* kinase assay (B, right panel). The remaining cells were treated with M-CSF (10 ng/ml) in the absence or presence of RANKL (100 ng/ml) for 4 days and then stained for TRAP (C). Percent cell survival was estimated by counting the relative number of cells in 15 independent fields (C, top panels). IP, immunoprecipitation; DAPI, 4′,6-diamidino-2-phenylindole.

M-CSF provided a physiological system to determine whether TAK1 deficiency affects RANKL-mediated signaling and osteoclast differentiation. In response to RANKL, activation of IKKβ induces the phosphorylation of IκBα, which results in its ubiquitination and degradation by the proteasome, thereby allowing nuclear translocation of the transcription factor NF-κB (3). As illustrated by defective phosphorylation and degradation of IκBα (Fig. 3D), IKK activation in response to RANKL is defective in TAK1$^{\Delta M}$-TNFR1$^{-/-}$ BMMs compared to control BMMs. Following stimulation with RANKL, TAK1$^{\Delta M}$-TNFR1$^{-/-}$ BMMs but not control BMMs also failed to activate JNK and the phosphorylation of c-Jun and p38 (Fig. 3D). Similar results were observed in TAK1$^{\Delta M}$-TNFR1$^{-/-}$ BMMs stimulated with lipopolysaccharide (LPS) (data not shown). Activation of IKK and therefore phosphorylation and degradation of IκBα are essential signaling events for RANKL-induced osteoclast differentiation since IKKβ-deficient BMMs do not form osteoclasts *in vitro* in response to RANKL (9, 10). As expected from the defective IKK signaling event, following treatment with M-CSF and RANKL, BMMs obtained from TAK1$^{\Delta M}$-TNFR1$^{-/-}$ mice did not form large, multinucleated TRAP^{+} osteoclasts, whereas BMMs derived from TAK1$^{F/+}$-TNFR1$^{-/-}$ mice did (Fig. 3E). Collectively, these results suggest that TAK1 is indispensable to activation of IKK and the stress kinases JNK and p38 by RANKL and that, as a result, loss of TAK1 significantly impairs osteoclast differentiation (Fig. 3F).

Loss of TAK1 potentiates spontaneous apoptosis and necroptosis in BMMs. Because simultaneous deletion of TNFR1 and TAK1 enabled the survival of BMMs in the presence of M-CSF, we next sought to determine whether the type of cell death occurring in TAK1$^{\Delta M}$ monocytes was apoptosis or necroptosis, the pathways of which are both activated by TNFR1 (33). Therefore, to examine whether apoptosis was occurring in the TAK1$^{\Delta M}$ monocytes, we immunoblotted cell lysates for the cleavage of caspase-8 and caspase-3 and for the disappearance of poly(ADP-ribose) polymerase (PARP). We found that lysates from TAK1$^{\Delta M}$ monocytes harvested from cultures on day 2 had cleaved caspase-8 and caspase-3 and lacked PARP and cells showed morphologies of membrane blebbing (Fig. 4A), all of which are indicators of apoptotic cell death. Because caspase-8 and capase-3 were activated in TAK1$^{\Delta M}$ monocytes, we next sought to determine whether zVAD-fmk, a broad-spectrum caspase inhibitor, could rescue the survival of these cells. Surprisingly, we found that instead of protecting the TAK1$^{\Delta M}$ monocytes from cell death, treatment with the caspase inhibitor resulted in a high death rate of TAK1$^{\Delta M}$ monocytes; furthermore, zVAD-fmk had no obvious cytotoxic effects on TAK1$^{F/+}$ monocytes (Fig. 4B). These results suggest that apoptosis is not the only mode of cell death in TAK1-deficient monocytes.

Because caspase inhibition did not protect all TAK1-deficient monocytes from cell death, we hypothesized that necroptosis, which is caspase independent (34), also causes cell death in TAK1-deficient monocytes. One of the hallmarks of necroptosis is loss of membrane integrity, which can be visualized through the uptake of cationic dyes such as PI. After TAK1$^{F/+}$ and TAK1$^{\Delta M}$ monocytes were cultured for 32 h in the presence of M-CSF, more TAK1$^{\Delta M}$ monocytes than TAK1$^{F/+}$ monocytes showed PI uptake

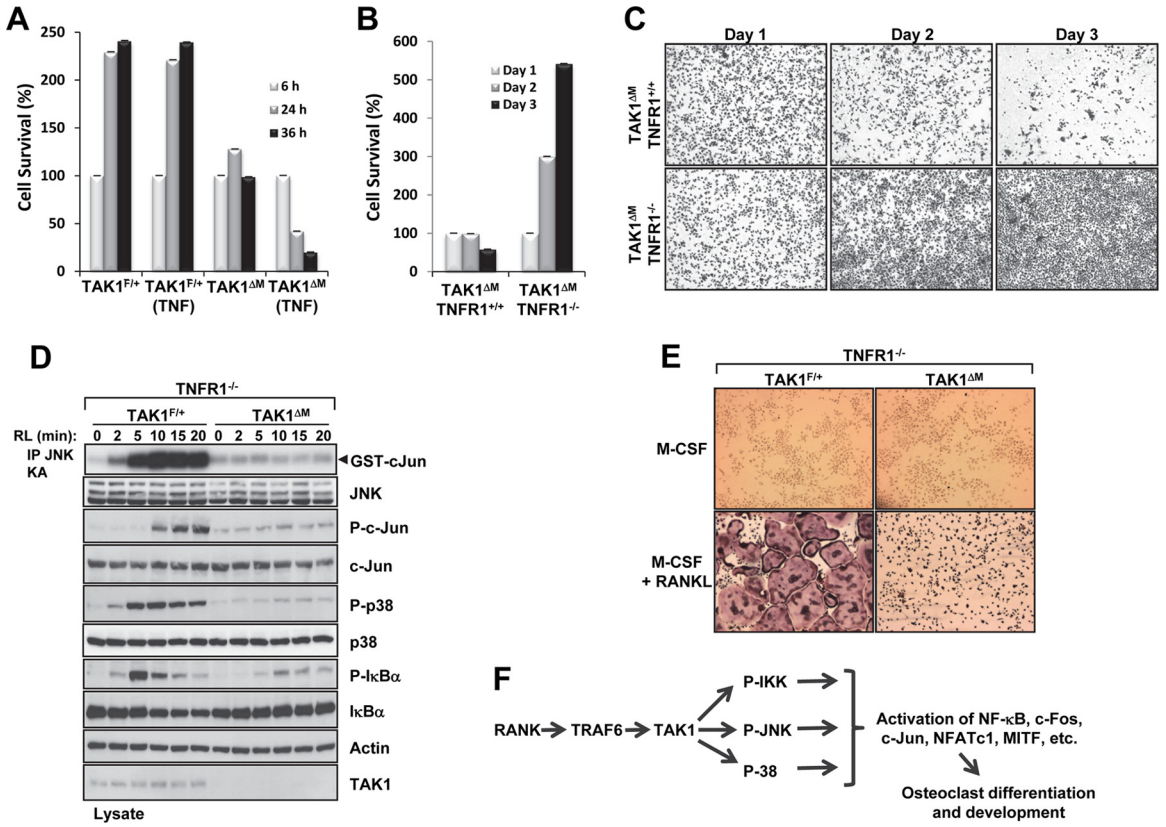

FIG 3 Survival of TAK1-deficient BMMs is rescued by deletion of TNFR1, and TAK1 is indispensable to osteoclast formation. (A) TAK1$^{\Delta M}$ BMMs are sensitive to TNF-α-induced cell death. TAK1$^{F/+}$ and TAK1$^{\Delta M}$ BMMs were treated with M-CSF (10 ng/ml) in the absence or presence of TNF-α (10 ng/ml), and cell survival was measured using the XTT assay. (B and C) TAK1$^{\Delta M}$ BMMs with or without TNFR1 deletion were lifted from the plate on the morning of day 1, counted, and replated at low density. Cell survival was measured using the XTT assay (B), and the cells were fixed and stained with crystal violet (C). (D) TAK1-deficient monocytes on a TNFR1-null background did not respond to RANKL (RL) treatment. BMMs from TAK1$^{\Delta M}$-TNFR1$^{-/-}$ or TAK1$^{F/+}$-TNFR1$^{-/-}$ mice were stimulated with RANKL (100 ng/ml), cell lysates were immunoblotted as indicated, and an *in vitro* kinase assay for JNK activity was performed. (E) BMMs derived from TAK1$^{\Delta M}$-TNFR1$^{-/-}$ or TAK1$^{F/+}$-TNFR1$^{-/-}$ mice were cultured in the presence of M-CSF (10 ng/ml) with or without RANKL (100 ng/ml) for 4 days, fixed, and stained for TRAP. (F) Schematic of the role of TAK1 in regulating RANKL signaling and osteoclast differentiation.

(Fig. 4C and D). The higher percentage of PI-positive TAK1$^{\Delta M}$ monocytes and the fact that caspase inhibition potentiated TAK1$^{\Delta M}$ monocyte death suggest that necroptosis also contributes to TAK1$^{\Delta M}$ monocyte death.

We then sought to confirm that necroptosis was one of the modes of death observed in TAK1$^{\Delta M}$ monocytes. RIP1, a key kinase in the initiation of caspase-independent cell death, can be inhibited by treatment with Nec-1, which allosterically blocks the kinase activity of RIP1, thereby preventing necroptosis (35, 36). We found that although treatment with zVAD-fmk did not protect TAK1$^{\Delta M}$ monocytes from cell death, treatment with Nec-1 did (Fig. 4E). These data indicate that the loss of TAK1 in monocytes results in two forms of cell death, apoptosis and necroptosis, and that these forms of cell death are prevented by the deletion of TNFR1 or blockade of the kinase activity of RIP1.

TAK1-KO MEFs are hypersensitive to TNF-induced cell death. Elucidating the components of the molecular machinery responsible for the death of TAK1-deficient monocytes is technically challenging because these cells die quickly *in vitro*. Therefore, to investigate the mechanisms of cell death, we generated TAK1-KO MEFs and confirmed their inability to activate IKK, JNK, and p38 in response to TNF-α (Fig. 5A) as previously reported (11, 12, 37). We found that following treatment with TNF-α, TAK1-KO MEFs were highly sensitive to cell death over 9 h in a dose-dependent manner (Fig. 5B).

We next determined whether the kinase activity of TAK1 was required to prevent TNF-α-induced cell death. Using a retroviral approach, we stably expressed FLAG-tagged TAK1 or a catalytically inactive mutant of TAK1 (TAK1-K63A) in TAK1-KO MEFs. Reconstituting TAK1-KO MEFs with TAK1, but not TAK1-K63A or empty vector (pMX), restored the degradation of IκBα in response to TNF-α and the cell viability in the presence of TNF-α (Fig. 5C and D). We also found that L929 cells expressing GFP-TAK1-C100, a fusion protein containing the C-terminal part of TAK1 that blocks the constitutive interaction of TAK1 with TAB2 and prevents TNF-α, interleukin-1β (IL-1β), and RANKL signaling to IKK and the stress kinases (20), were highly sensitive to TNF-α-induced cell death (Fig. 5E). Collectively, these results indicate that TAK1 deficiency, a catalytically inactive mutant of TAK1, or blockade of the constitutive interaction of TAK1 and TAB2 results in hypersensitivity to TNF-α-induced cell death.

TNF-α induces both apoptosis and necroptosis in TAK1-KO MEFs. For TNFR1 to induce cell death, RIP1 must dissociate from the survival complex I and induce the formation of the death-inducing complex (complex II) by offering a docking surface for Fas-associated death domain (FADD) and caspase-8 or for FADD

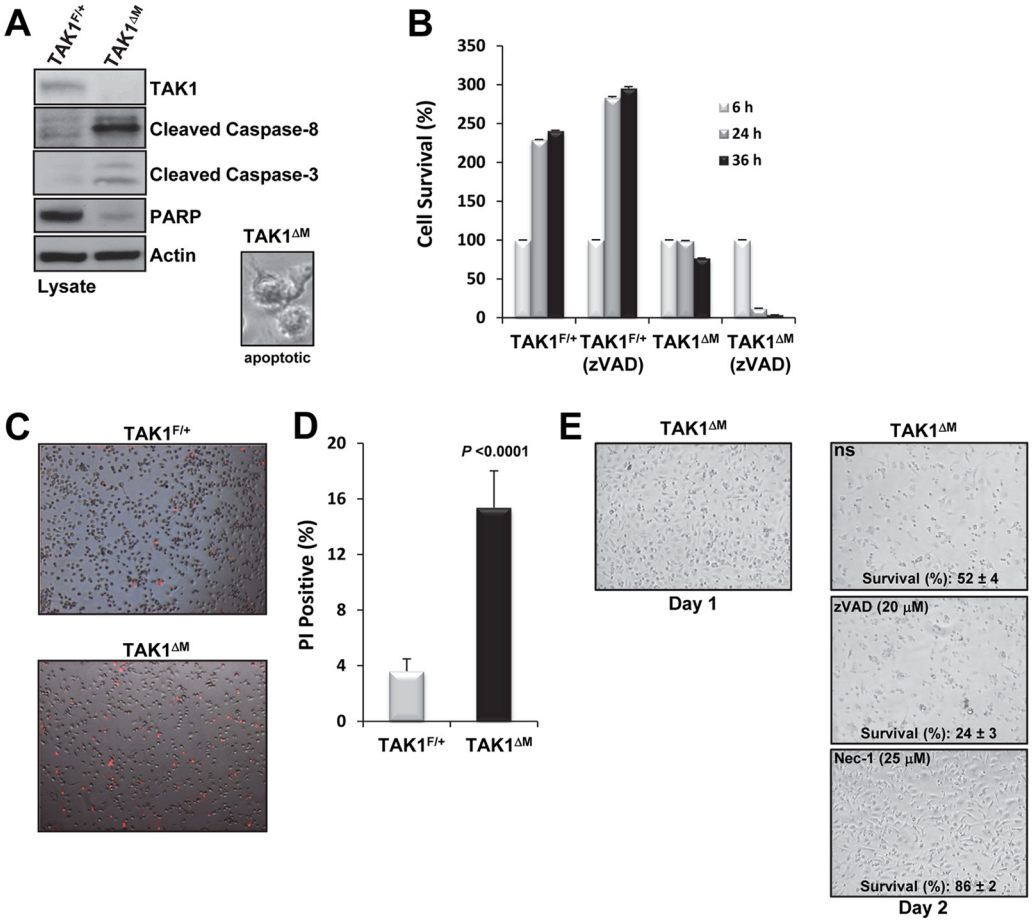

FIG 4 TAK1-deficient BMMs die by apoptosis and necroptosis. (A) Active caspases in TAK1-deficient monocytes. $TAK1^{F/+}$ and $TAK1^{\Delta M}$ BMMs were harvested on the morning of day 2, and protein lysates were immunoblotted as indicated. A representative phase-contrast image of an apoptotic cell is shown (inset). (B) zVAD-fmk potentiates the cell death of TAK1-deficient monocytes. On the morning of day 1, $TAK1^{F/+}$ and $TAK1^{\Delta M}$ BMMs were lifted from the plate, counted, and replated at high density in the absence or presence of zVAD-fmk (10 μM). Cell survival was measured using the XTT assay. (C and D) On the morning of day 2, $TAK1^{F/+}$ and $TAK1^{\Delta M}$ BMMs were stained with PI (C), and the percentage of PI-positive cells was measured (D). (E) Nec-1 treatment protects TAK1-deficient monocytes from cell death. Representative phase-contrast images and percent survival of $TAK1^{\Delta M}$ BMMs after 36 h of treatment with M-CSF (10 ng/ml) in the presence of either zVAD-fmk or Nec-1 are shown.

and RIP3 to initiate apoptosis or necroptosis, respectively (34, 36). In TAK1-KO MEFs, interaction between RIP1 and FADD occurred rapidly in response to TNF-α (Fig. 6A). Notably, treatment with TNF-α for 2 or 3 h caused significant loss of full-length RIP1, likely because of its cleavage by active caspases (Fig. 6A). In addition, the FADD-RIP1 interaction was significantly attenuated in TAK1-KO MEFs reconstituted by retroviral delivery of TAK1 but not TAK1-K63A (Fig. 6B).

Moreover, zVAD-fmk did not prevent the TNF-α-induced death of TAK1-KO MEFs (Fig. 7A); however, immunoblotting for cleaved caspase-3 confirmed zVAD-fmk's capacity to prevent caspase cleavage (Fig. 7B). We observed similar results in TAK1-KO MEFs treated with the caspase-8 inhibitor zIEDT-fmk (data not shown). Surprisingly, treatment with Nec-1 not only protected the TAK1-KO MEFs from TNF-α-induced cell death (Fig. 7A) but also attenuated caspase-3 cleavage (Fig. 7B) and RIP1-FADD interaction in these cells (Fig. 7C). Similarly, treatment with Nec-1 and zVAD-fmk protected TAK1-KO MEFs from TNF-α-induced cell death (Fig. 7A) and caspase-3 cleavage (Fig. 7B). In the presence of TNF-α, TAK1-KO MEFs revealed an increase of PI-positive necrotic cells that was enhanced in the presence of zVAD-fmk but considerably attenuated in the presence of Nec-1 or Nec-1 plus zVAD-fmk (Fig. 7D). These results indicate that in TAK1-KO MEFs, TNF-α treatment causes the rapid association of RIP1 with FADD, caspase cleavage, and loss of membrane integrity and that treatment with Nec-1 in the presence or absence of zVAD-fmk protects these cells against TNF-α-induced cell death.

Knockdown of RIP3 protects against TNF-α-mediated necroptosis but not apoptosis in TAK1-KO MEFs. Because RIP1 and RIP3 form a complex in which they are phosphorylated and activated to engage TNF-α-induced necroptosis, we next investigated the effect of silencing RIP3 on TNF-α-induced cell death in TAK1-KO MEFs. To generate the stable knockdown of RIP3 in TAK1-KO MEFs, we used a lentivirus expressing an shRNA-targeting RIP3 (shRIP3) (38–40); an shRNA-targeting luciferase (shLuc) was used as the negative control (Fig. 8A). As expected, shLuc did not protect TAK1-KO MEFs from TNF-α-induced cell death (Fig. 8B). The cell morphologies were indicative of apoptosis (cells with membrane blebs) and necroptosis (rounded, ne-

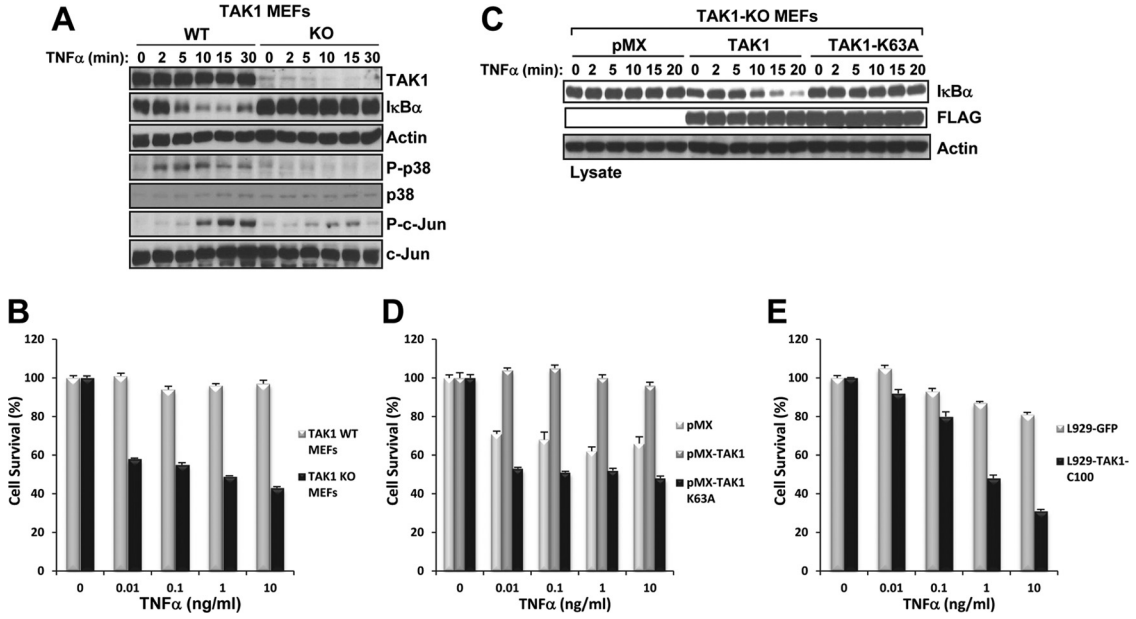

FIG 5 TAK1-KO MEFs have defective TNF-α signaling and are hypersensitive to TNF-α-induced cell death. (A) WT and TAK1-KO MEFs were stimulated with TNF-α (10 ng/ml), and the cell lysates were immunoblotted with the indicated antibodies. (B) WT and TAK1-KO MEFs plated in 96-well plates were treated with TNF-α for 9 h, and cell viability was assessed using crystal violet staining. (C and D) TAK1-KO MEFs expressing empty vector (pMX), TAK1, or TAK1-K63A were stimulated with TNF-α (10 ng/ml) as indicated, and the cell lysates were immunoblotted with the indicated antibodies (C). The indicated cells were plated in 96-well plates and treated with TNF-α for 9 h, and cell viability was assessed using crystal violet staining (D). (E) L929 cells expressing GFP-TAK1-C100 are hypersensitive to TNF-α-induced cell death. L929 cells expressing GFP or GFP-TAK1-C100 were plated in a 96-well plate and treated with TNF-α for 9 h, and cell viability was assessed using crystal violet staining.

crotic cell-like cells) (Fig. 8D, column b, bottom inset), which were confirmed by the presence of caspase-3 cleavage (Fig. 8C) and PI-positive staining (Fig. 8D, column b), respectively. Treating these cells with zVAD-fmk blocked TNF-α-induced caspase-3 cleavage (Fig. 8C), resulting in necroptosis, as indicated by necrotic cell morphology (Fig. 8D, column c, bottom inset) and enhanced PI-positive staining (Fig. 8D, column c). TAK1-KO MEFs expressing shRIP3 were sensitive to TNF-α-induced cell death (Fig. 8B), but the death was exclusively apoptotic, as indicated by apoptotic cell morphology (Fig. 8D, column e, bottom inset), chromatin condensation (Fig. 8D, column e, Hoechst), the absence of PI-positive staining (Fig. 8D, column e), and the pres-

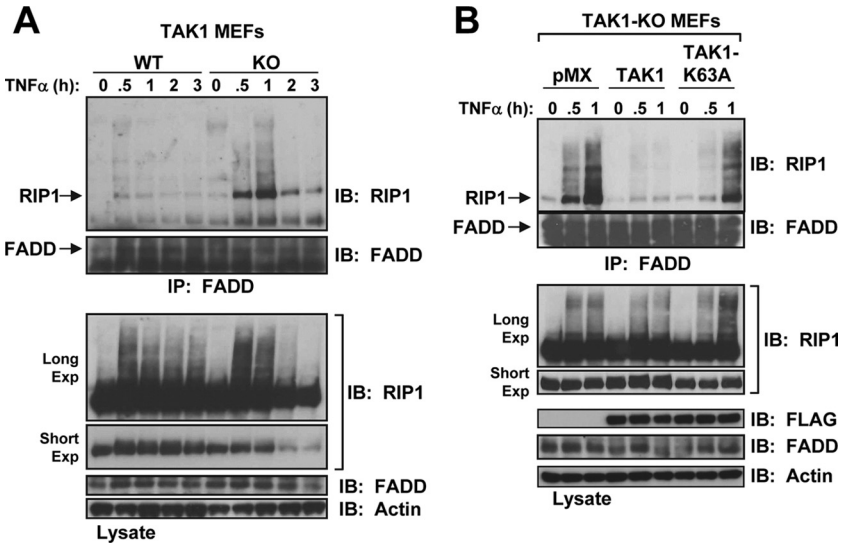

FIG 6 RIP1 forms a complex with FADD in TAK1-KO MEFs in response to TNF-α. (A) WT and TAK1-KO MEFs were stimulated with TNF-α (10 ng/ml), and the cell lysates were immunoprecipitated with an anti-FADD antibody and immunoblotted with anti-RIP1 (top) or anti-FADD (bottom). The cell lysates were immunoblotted with the indicated antibodies (Long Exp, long exposure; Short Exp, short exposure). (B) Reconstitution of TAK1-KO MEFs with TAK1 but not TAK1-K63A blocks FADD and RIP1 interaction in response to TNF-α. TAK1-KO MEFs expressing empty vector (pMX), TAK1, or TAK1-K63A were processed as described for panel A.

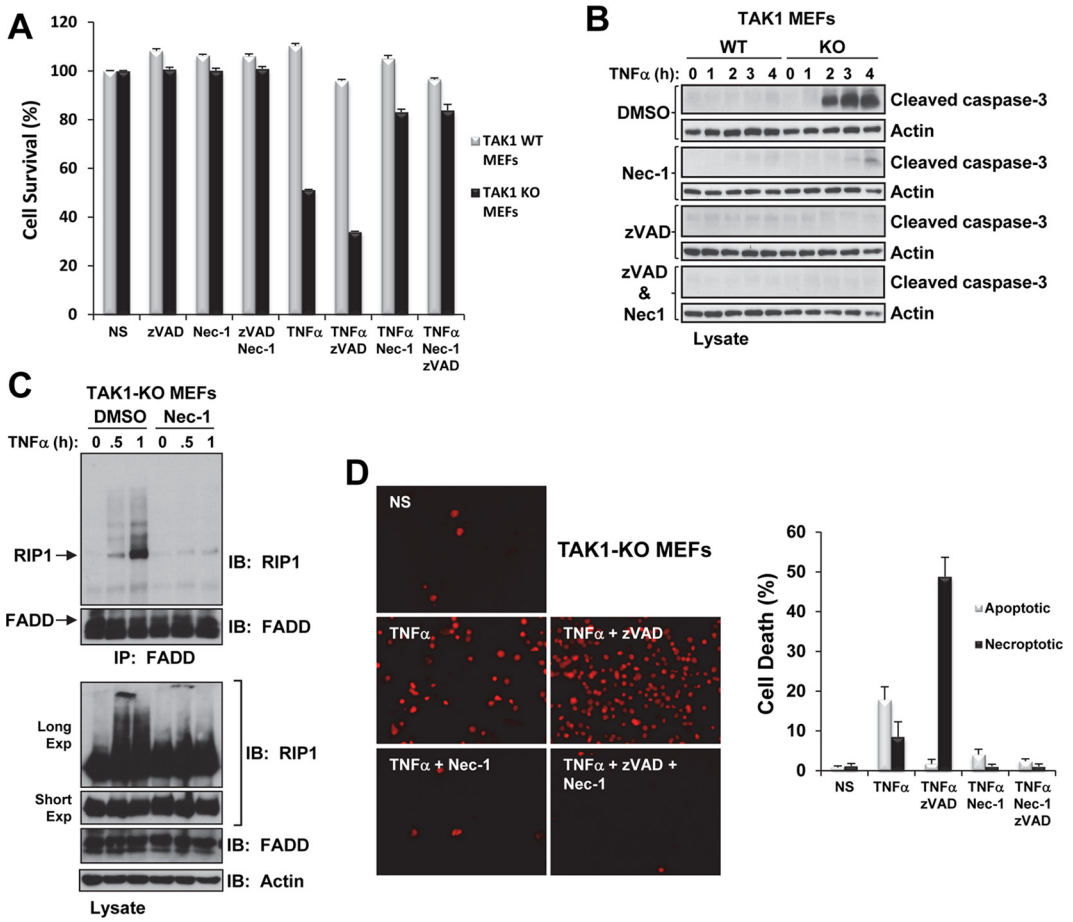

FIG 7 Nec-1 prevents TNF-α-induced cell death of TAK1-KO MEFs. (A) WT and TAK1-KO MEFs were pretreated for 30 min with zVAD-fmk (20 μM) and/or Nec-1 (50 μM) and then treated with TNF-α (1 ng/ml) for 9 h. Cell viability was assessed using crystal violet staining. NS, nonstimulated. (B) WT and TAK1-KO MEFs were pretreated for 30 min with combinations of dimethyl sulfoxide (DMSO) (1%), zVAD-fmk (20 μM), or Nec-1 (50 μM) as indicated and then treated with TNF-α (1 ng/ml). The cell lysates were immunoblotted with the indicated antibodies. (C) TAK1-KO MEFs were pretreated for 30 min with DMSO (1%) or Nec-1 (50 μM) and then treated with TNF-α (10 ng/ml). The cell lysates were processed as described in the Fig. 6A legend. (D) TAK1-KO MEFs were pretreated as described for panel A, treated with TNF-α (1 ng/ml) for 1 h 45 min, and then stained with PI. Representative images of fluorescent PI-positive TAK1-KO MEFs under the indicated treatment conditions (left) and the percentage of cell death attributed to apoptosis (chromatin condensation) and necroptosis (PI positive) (graph, right) are shown.

ence of caspase-3 cleavage (Fig. 8C). zVAD-fmk treatment abolished the TNF-α-induced apoptosis of shRIP3 TAK1-KO MEFs (Fig. 8B), as indicated by the absence of caspase-3 cleavage (Fig. 8C) and normal cell morphology (Fig. 8D, column f). The results depicted above were based on knockdown using a single shRNA-targeting RIP3. Taken together, these results suggest that TNF-α induces two forms of cell death in the absence of TAK1; furthermore, if the apoptotic pathway is inhibited, the necroptotic pathway becomes the major contributor to cell death, and vice versa (Fig. 8E).

TAK1 is required for osteoclastogenesis *in vivo*. The conditional deletion of TAK1 in osteoclast precursors confirmed that TAK1 is required for RANKL-induced signaling events and consequently for osteoclast differentiation *in vitro*. We next sought to identify the physiological consequence of TAK1 loss in osteoclasts *in vivo*. The Ctsk-Cre knock-in line (22) has been used to delete genes in the osteoclast lineage, including *ER*α (22), *CDC42* (41), *Bcl-x*$_L$ (42), *NIK* (43), *Dicer* (44), *Blimp1* (45), and *Rac1/2* (46). Therefore, we crossed TAK1-floxed mice with Ctsk-Cre mice to generate littermates that were wild type (TAK1$^{+/+}$-Ctsk$^{Cre/+}$; TAK1$^{+/+}$) or heterozygote (TAK1$^{F/+}$-Ctsk$^{Cre/+}$; TAK1$^{F/+}$) or had a deletion of TAK1 in osteoclasts (TAK1$^{F/-}$-Ctsk$^{Cre/+}$; TAK1$^{\Delta OC}$). To anticipate any potential cytotoxicity effect of TNF-α, we generated in parallel TAK1$^{\Delta OC}$ mice on a TNFR1-null background.

Consistent with previous reports (28, 31, 47), we did not observe any differences between wild-type or heterozygote mice. The TAK1$^{\Delta OC}$ pups were born at the expected Mendelian ratio and were indistinguishable from their littermates at birth until about 3 days. Surprisingly, the TAK1$^{\Delta OC}$ pups were 50% smaller than their littermates at 5 to 7 days, had dry, thick, hard, scaly skin (Fig. 9A), and died between 1 and 8 days. The survival of TAK1$^{\Delta OC}$ pups was extended for approximately 1 week longer on a TNFR1-null background, but these mice eventually died at about 15 days (Fig. 9A), suggesting that TNFR1 was partially involved in the death of the TAK1$^{\Delta OC}$ mice.

The cathepsin K gene is a RANKL-inducible gene that is expressed approximately 2 days after RANKL treatment *ex vivo*; therefore, in the Ctsk-Cre model, gene deletion occurs during

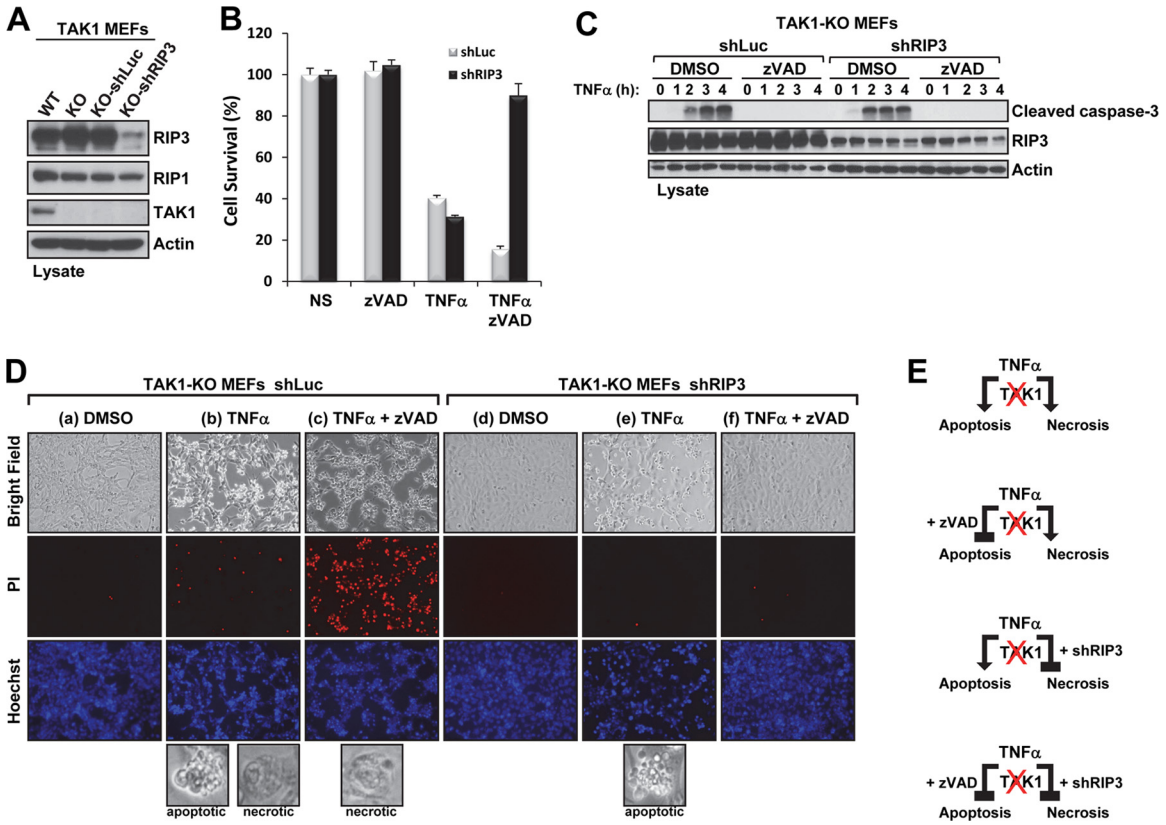

FIG 8 Stable knockdown of RIP3 combined with caspase inhibition protects TAK1-KO MEFs from TNF-α-induced cell death. (A) The indicated cell lysates were immunoblotted with the indicated antibodies. (B and C) TAK1-KO MEFs infected with shRNA-luciferase (shLuc) or shRNA-RIP3 (shRIP3) were pretreated for 30 min with dimethyl sulfoxide (DMSO) (1%) or zVAD-fmk (20 μM) and then treated with TNF-α (1 ng/ml) for 9 h. Cell viability was measured using the CellTiter-Glo assay (B). TAK1-KO MEFs expressing shLuc or shRIP3 were pretreated as described for panel B and treated with TNF-α (1 ng/ml) for the indicated times, and the cell lysates were immunoblotted with the indicated antibodies (C). (D) TAK1-KO MEFs expressing shLuc or shRIP3 were pretreated with DMSO (1%; columns a, b, d, and e) or zVAD-fmk (20 μM; columns c and f) for 30 min, stimulated with TNF-α (1 ng/ml; columns b, c, e, and f) for 1 h 45 min, and then stained with PI (red) and Hoechst (blue). Representative phase-contrast and fluorescence microscopy images (magnification, ×10) of the cells under the indicated treatment conditions are shown. The bottom panels in columns b, c, and e show images (magnification, ×20) of cells dying by apoptosis (as indicated by membrane blebs) or by necroptosis (as indicated by rounded, necrosis-like morphology). (E) Schematic of TNF-α-induced cell death in TAK1-deficient MEFs.

osteoclast differentiation (22), which is different from that in the LysM-Cre model. M-CSF splenic-derived monocytes from $TAK1^{\Delta OC}$ and $TAK1^{+/+}$ pups had similar levels of TAK1 expression (Fig. 9B). While both $TAK1^{\Delta OC}$ and $TAK1^{+/+}$ monocytes expressed Cre following RANKL stimulation, only $TAK1^{\Delta OC}$ osteoclast progenitors showed corresponding loss of the TAK1 protein after 48 and 72 h of RANKL treatment (Fig. 9B), confirming that the Ctsk-Cre line was deleting TAK1 in differentiating osteoclasts.

To determine whether osteoclast-specific deletion of TAK1 affects bone remodeling *in vivo*, we performed bone histomorphometry analysis on a cohort of 6-day-old $TAK1^{\Delta OC}$ mice and 10-day-old $TAK1^{\Delta OC}$-$TNFRI^{-/-}$ mice and their control littermates. Histochemical staining for TRAP, a widely used osteoclast marker, revealed that the femoral section of the long bones of $TAK1^{\Delta OC}$ mice had fewer $TRAP^{+}$ cells than that of $TAK1^{+/+}$ mice did (Fig. 9C, upper panels). In contrast, the femoral sections of $TAK1^{\Delta OC}$-$TNFRI^{-/-}$ mice showed the presence of $TRAP^{+}$ staining (Fig. 9C, bottom panels), but unlike what was seen in their littermate controls, the majority of the osteoclasts appeared in the proximal metaphysis region and very few were in the regions of the cortical bone (Fig. 9D). Whether in the presence or absence of TNFR1, bone histomorphometry analysis of $TAK1^{\Delta OC}$ mice revealed a severe increase in bone volume that was likely due to the higher trabecular number and decreased trabecular spacing and likely reflects the severe osteoclast defects and the decrease in osteoclastic bone resorption parameters (Fig. 9E). Collectively, these data suggest that $TAK1^{\Delta OC}$ mice had a severe osteopetrotic phenotype and TAK1 plays a critical role in regulating survival and osteoclastogenesis *in vivo*.

Osteoclast-specific deletion of TAK1 impairs osteoclast differentiation and resorption activity *in vitro*. As stated earlier, in the Ctsk-Cre model, cathepsin K expression occurs between 24 and 48 h following treatment with RANKL and coincides with Cre expression. Using the Ctsk-Cre model to study the role of a protein during osteoclast development *in vitro* is challenging because Cre expression in the fusing cells may not be synchronous (46). Nevertheless, we used this model to investigate the role of TAK1 during osteoclast differentiation. Treating $TAK1^{+/+}$ monocytes with M-CSF and RANKL caused the formation of large, multinucleated $TRAP^{+}$ osteoclasts, whereas the same treatment of $TAK1^{\Delta OC}$ monocytes caused the formation of fewer osteoclasts

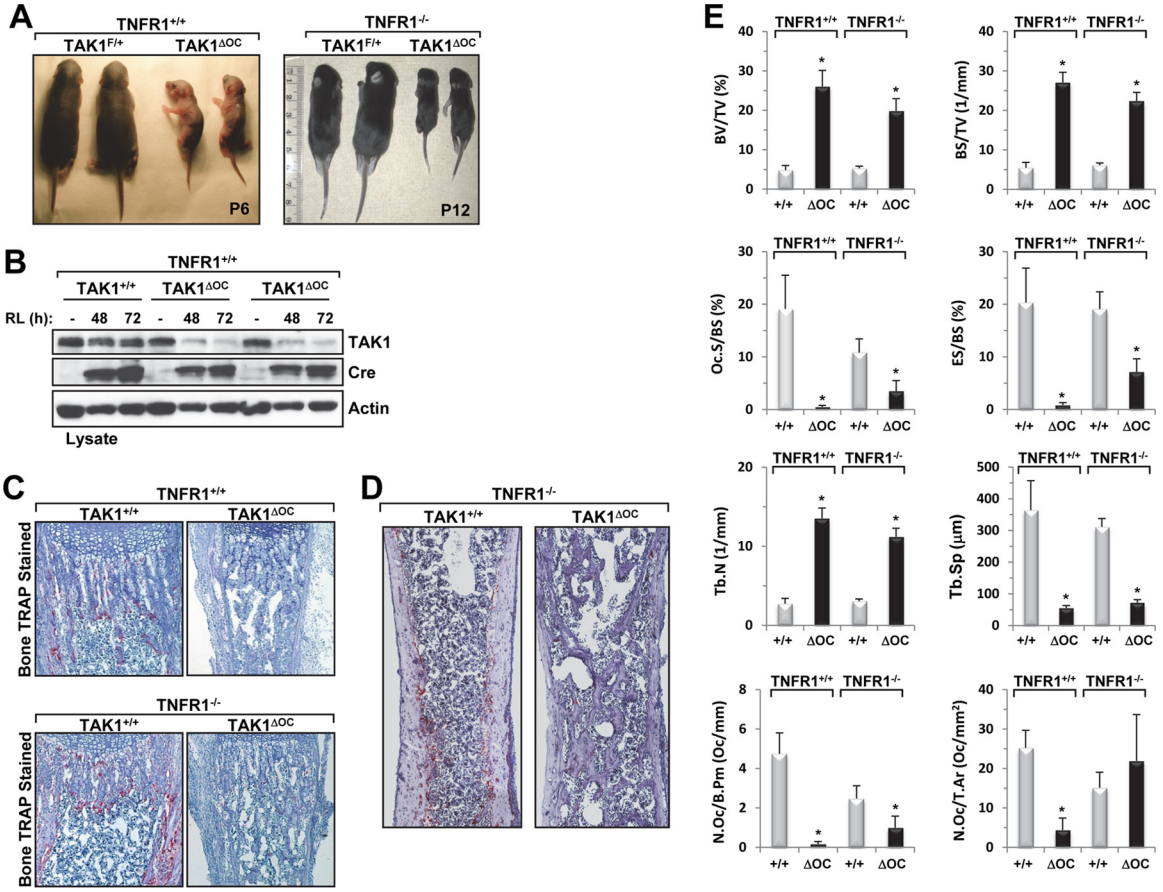

FIG 9 Conditional deletion of TAK1 in osteoclasts results in growth retardation, postnatal lethality, and severe osteopetrosis in TAK1$^{\Delta OC}$ mice. (A) Growth retardation of TAK1$^{\Delta OC}$ pups. Photographs of 6-day-old TAK1$^{\Delta OC}$ mice and 12-day-old TAK1$^{\Delta OC}$-TNFR1$^{-/-}$ mice with their respective control littermates. (B) RANKL-induced loss of TAK1 expression in TAK1$^{\Delta OC}$ differentiating osteoclasts. TAK1$^{+/+}$ and TAK1$^{\Delta OC}$ spleen-derived monocytes were cultured with M-CSF (10 ng/ml) in the absence or presence of RANKL (RL, 100 ng/ml), and the cell lysates were immunoblotted with the indicated antibodies. (C) Representative images of TRAP-stained osteoclasts (red) in the femurs of the indicated mice (magnification, ×40). (D) Representative images of TRAP-stained sections in the femurs of the indicated mice. (E) Results of the histomorphometric analysis of femurs from 6-day-old male TAK1$^{+/+}$-TNFR1$^{+/+}$ mice ($n = 4$), 6-day-old male TAK1$^{\Delta OC}$-TNFR1$^{+/+}$ mice ($n = 5$), 10-day-old male TAK1$^{+/+}$-TNFR1$^{-/-}$ mice ($n = 5$), and 10-day-old TAK1$^{\Delta OC}$-TNFR1$^{-/-}$ mice ($n = 5$). BV/TV, bone volume per total volume; BS/TV, bone surface per total volume; Tb.N, trabecular number; Tb.Sp, trabecular spacing; Oc.S/BS, percentage of bone surface covered with osteoclasts; ES/BS, percentage of bone surface eroded by osteoclasts; N.Oc/B.Pm, number of osteoclasts per bone perimeter; N.Oc/T.Ar, number of osteoclasts per tissue area of interest. *, $P < 0.001$.

(Fig. 10A) that was likely due to impaired RANKL signaling (Fig. 10B). The osteoclasts that did form were smaller and had dysfunctional morphologies (Fig. 10C, top right panel) and an impaired capacity to resorb bone (Fig. 10C, bottom right panel). Similar characteristics, including the formation of fewer osteoclasts (data not shown) and the presence of spikelike projections (Fig. 10D, bottom panel), were observed in osteoclasts differentiated from TAK1$^{\Delta OC}$-TNFR1$^{-/-}$ splenic monocytes *in vitro*. The surface area covered by and the number of nuclei in TAK1$^{\Delta OC}$ osteoclasts (data not shown) and TAK1$^{\Delta OC}$-TNFRI$^{-/-}$ osteoclasts were significantly smaller than those of the control osteoclasts (Fig. 10E and F). TAK1$^{\Delta OC}$-TNFR1$^{-/-}$ osteoclasts also had impaired resorption activity *in vitro* (Fig. 10G). The spikelike projections on, the small size of, and fewer nuclei in TAK1$^{\Delta OC}$ and TAK1$^{\Delta OCS}$-TNFRI$^{-/-}$ osteoclasts suggest that the fusion of the osteoclast progenitors was incomplete. Together, these results indicate that differentiating osteoclasts require TAK1 to develop into large, multinucleated osteoclasts capable of resorbing bone, which is consistent with the severe osteopetrotic phenotype observed in the TAK1$^{\Delta OC}$ mice.

DISCUSSION

In the present study, we found that TAK1 expression was required to prevent TNFR1-induced cell death by apoptosis and necroptosis in BMMs. The spontaneous cell death of TAK1-deficient monocytes could not be rescued by treatment with increasingly large amounts of M-CSF or by caspase inhibition, which in fact caused greater cell death. Only prevention of RIP1 kinase activity with Nec-1, retroviral delivery of TAK1, or genetic deletion of TNFR1 rescued the TAK1-deficient monocytes from spontaneous cell death. Additional investigation revealed that the simultaneous inhibition of caspases and knockdown of RIP3 completely blocked TNF-α-induced cell death in TAK1-KO MEFs. TAK1-deficient osteoclast precursors rescued from programmed cell death indicated that TAK1 has an indispensable role in RANKL-induced osteoclastogenesis *in vitro*. Furthermore, deletion of

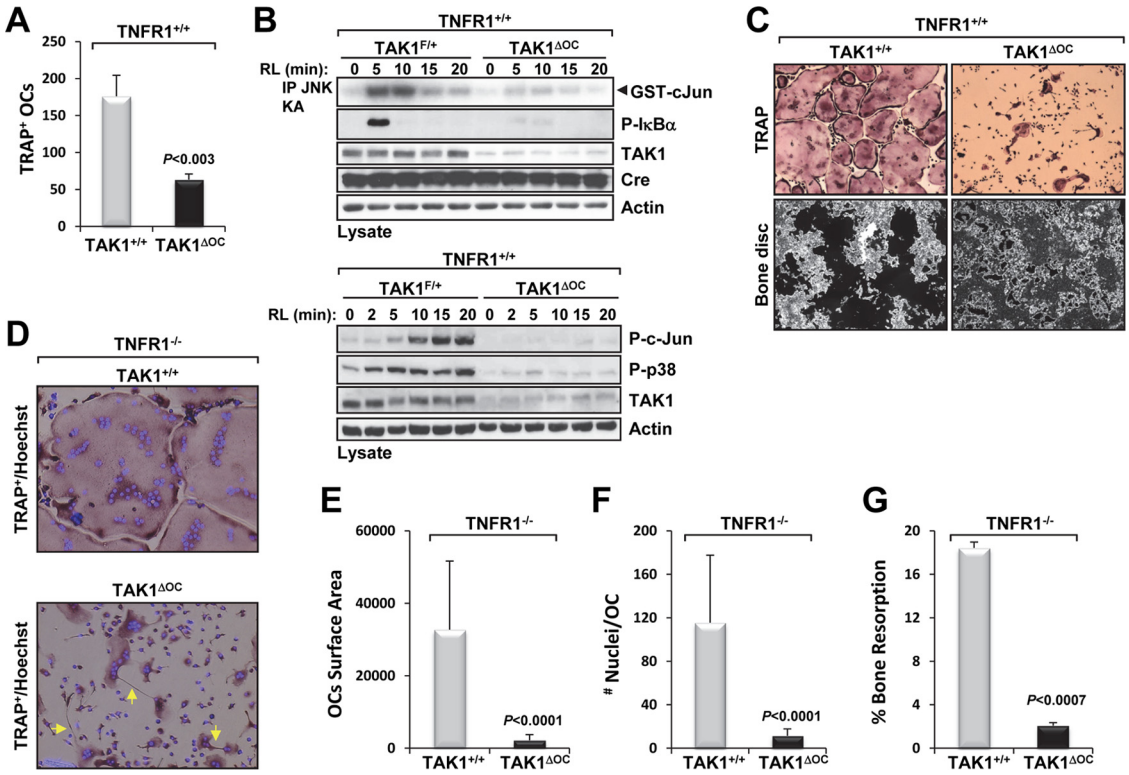

FIG 10 *Ex vivo* analysis of TAK1$^{\Delta OC}$ osteoclast formation and resorption activity. (A) TAK1$^{\Delta OC}$ osteoclast development is defective. Spleen-derived monocytes from TAK1$^{+/+}$ and TAK1$^{\Delta OC}$ mice were treated with M-CSF (10 ng/ml) and RANKL (100 ng/ml) for 72 h on plastic dishes or bone discs. Cells were stained for TRAP, and multinucleated TRAP^{+} cells were quantified. (B) TAK1$^{\Delta OC}$ osteoclasts did not respond to RANKL treatment. Spleen-derived monocytes from the indicated mice were treated as described for panel A, starved for 2 h followed by RANKL (RL, 100 ng/ml) treatment for the indicated times, and processed as described in the legend to Fig. 3D. (C) Representative images of TRAP staining (top panels) and bone resorption (black areas, bottom panels) (magnification, ×10) are shown. (D to G) TAK1$^{\Delta OC}$-TNFR1$^{-/-}$ differentiating osteoclasts have defects similar to those of TAK1$^{\Delta OC}$-TNFR1$^{+/+}$ osteoclasts. Spleen-derived monocytes were treated as described for panel A on plastic dishes (D to F) or bone discs (G). Representative images of TRAP and Hoechst staining (magnification, ×20) are shown with yellow arrows pointing at spikelike projections (D). Graphic representations of the area occupied by osteoclasts (E), the number of nuclei per osteoclast (F), and the percent bone resorption (G) are shown.

TAK1 in osteoclasts revealed that TAK1 is essential to osteoclast survival, development, and function *in vivo*. Together, these findings indicate that TAK1 is essential for osteoclast differentiation and an important modulator of cell death by apoptosis and necroptosis. The results of the present study have clearly solidified the foundation for the RANK-TRAF6-TAK1-IKK signaling axis in osteoclast biology.

The fact that BMMs deficient in IKKβ, a major kinase activated by TAK1 in the NF-κB pathway, do not undergo spontaneous cell death (9, 10) suggests that the protective effects of TAK1 are independent of its ability to activate NF-κB. Rather, TAK1 is an important modulator that prevents the rapid formation of the death-inducing signaling complex critical to the execution of apoptosis and necroptosis. A similar postulate for RIP1 with a defective ubiquitination site in response to TNF-α has been reported (48). Likewise, the second mitochondrion-derived activator of caspase (SMAC) mimetic-induced loss of cellular inhibitor of apoptosis proteins, which are responsible for RIP1 ubiquitination in the survival TNFR1 complex I, results in TNFR1-induced necroptosis in BMMs (49). Our observation that caspase inhibition potentiated TAK1$^{\Delta M}$ monocyte cell death is consistent with those of Wu et al., who found that in some cell types, such as the murine fibrosarcoma line L929, treatment with zVAD-fmk blocked apoptotic cell death while sensitizing the cells to necroptosis (50). In L929 cells, blocking apoptosis with zVAD-fmk results in spontaneous sensitization to necroptosis, which depends on the autocrine production of TNF-α and the kinase activity of RIP1, though the exact mechanism by which it does so remains unclear (34, 50–52). Our findings suggest that loss of TAK1, a component of TNFR1 complex I, shifts the balance from the maintenance of complex I to the rapid formation of complex II, thereby promoting the self-destruction of the BMMs in a TNFR1-dependent manner.

Necroptosis, a mechanism of programmed necrotic cell death, can be blocked by Nec-1, an inhibitor of RIP1 kinase activity, which is believed to be exclusive for death by necroptosis (35). However, similar to Arslan and Scheidereit's findings (53), we observed that Nec-1 could significantly attenuate caspase cleavage and the interaction between RIP1 and FADD. Analogous to these observations, findings from Wang et al. indicated that RIP1's kinase activity is required for TNF-α–SMAC mimetic-induced apoptosis and the interaction of RIP1, FADD, and caspase-8 (54). On the basis of the notion that Nec-1 is exclusive to necroptosis and the fact that Nec-1 protects against the cytotoxic effects of TNF-α in the absence of TAK1, Arslan and Scheidereit concluded that TNF-α solely induces necroptosis in the absence of TAK1 (53). However, we found that knockdown of RIP3, the key player downstream of RIP1 in the execution of necroptosis, did not protect TAK1-KO MEFs against TNF-α-induced cell death; rather,

cell death continued exclusively by apoptosis (Fig. 8B and D). Together, these findings indicate that in TAK1-KO MEFs, the kinase activity of RIP1 is also involved in cell death by apoptosis; however, the way in which Nec-1 attenuates caspase cleavage and prevents RIP1-FADD formation remains unclear.

The expression of catalytically inactive TAK1 (TAK1-K63A) in TAK1-KO MEFs did not protect against TNF-α-induced cell death (Fig. 5D), which is inconsistent with the findings of Arslan and Scheidereit (53). This discrepancy could be explained by the fact that Arslan and Scheidereit used a single clone, whereas we used a pool of cells to avoid clonal artifacts. In addition, we found that in response to TNF-α, FADD forms a complex with RIP1 in TAK1-K63A cells as well as in TAK1-KO MEFs reconstituted with empty vector (Fig. 6). In agreement with our findings, in response to TNF-α, FADD has been found to interact with RIP1 following inhibition of TAK1 kinase activity with the kinase inhibitor 5Z-7-oxozeaenol (55), confirming that TAK1's kinase activity is required to prevent the formation of the FADD-RIP1 complex. Nevertheless, this raises the question of whether the phosphorylation of adaptor proteins involved in the formation of TNFR1 complex I causes a more stable complex that would prevent the formation of the death-inducing complex.

In addition, we found that when it is in a complex with FADD, RIP1 is significantly ubiquitinated. This observation, which is consistent with those of 2 previous studies (53, 56), challenges the current model, in which RIP1 must be deubiquitinated to leave the TNFR1 survival complex I and engage with FADD, caspase-8, and RIP3 in the death-inducing complex (48, 54). However, the nature of the lysine-linked polyubiquitin chain attached to RIP1 while in complex with FADD has yet to be determined. Pulldown of Lys63-polyubiquitinated proteins using glutathione *S*-transferase–TAB2-Zn finger (8) followed by immunoblotting with RIP1 revealed a significantly higher accumulation of the Lys63-linked ubiquitin chain on RIP1 in TAK1-KO MEFs than in WT MEFs between 15 and 90 min following TNF-α stimulation (data not shown). This finding suggests that RIP1 is ubiquitinated with Lys63-linked ubiquitin chains at about the same time it interacts with FADD in TAK1-KO MEFs; however, this experiment did not reveal the cellular location of RIP1.

The role of TAK1 as a TRAF6-activated downstream kinase in the IL-1R/TLR and B-/T-cell receptor pathways is well documented (11, 12, 30, 31, 47, 57). RANK binds several TRAFs; however, the severe osteopetrotic phenotype reported for TRAF6-deficient mice (5) indicates that TRAF6 is the major adaptor molecule of RANK-induced osteoclastogenesis. Our *in vitro* investigation of the role of TAK1 in RANKL-induced osteoclastogenesis revealed that in response to RANKL, TAK1-deficient monocytes, like TRAF6-deficient monocytes, failed to activate IKK, JNK, and p38 and did not form multinucleated osteoclasts (5, 7, 8). Importantly, the IKK and stress kinases have been implicated as critical RANK signaling intermediates in osteoclast differentiation (58). For example, both IKKβ- and JNK1-deficient BMMs showed impaired formation of osteoclasts *in vitro* (9, 10, 59) and selective inhibition of p38 kinase activity prevented RANKL-mediated osteoclast differentiation (60, 61). To our knowledge, ours is the first study in which primary TAK1-deficient osteoclast precursors were used to solidify the RANK-TRAF6-TAK1 signaling axis in osteoclastogenesis.

We used the Ctsk-Cre line to evaluate the physiological role of TAK1 in osteoclast development *in vivo* and were surprised to find that conditional deletion of TAK1 resulted in early postnatal death, which could be rescued (albeit for only 1 week) by simultaneous deletion of TNFR1. The postnatal death of $TAK1^{\Delta OC}$ mice in the present study raises the possibility that deletion of TAK1 was not sequestered to the osteoclast compartment; however, the cause of postnatal death remains unknown. Examination of the $TAK1^{\Delta OC}$ femurs, whether on a $TNFR1^{+/+}$ or $TNFR1^{-/-}$ background, revealed poor bone remodeling due to impaired osteoclast formation and activity indicative of a severe osteopetrotic phenotype. These findings are the first to indicate that TAK1 plays an essential role in osteoclast development *in vivo*.

Notably, the $TAK1^{\Delta OC}$ pups had hard, inflexible, scaly skin and rough skin around the lips in particular (Fig. 9A). This skin phenotype was surprisingly similar to that of mice in which TAK1 was deleted in epidermal tissue using the keratin 5-Cre line (28, 62). The presumed skin phenotype of the mice in the present study could be explained by the expression of cathepsin K in other cell types such as skin fibroblasts, lung, and epidermis (63–65). Currently, cathepsin K inhibitors are in clinical trials for the treatment of osteoporosis; skin problems have been reported in some patients (66), and studies of the long-term use of these drugs may reveal other side effects.

The last several years have seen a significant amount of research that has focused on TAK1's central role in regulating the NF-κB and stress kinase pathways through a variety of cytokines in different cell types and tissues. For instance, mice lacking TAK1 in the osteoblast lineage, the cells responsible for bone formation, showed defects in osteoblast differentiation as well as clavicular hypoplasia and delayed fontanelle closure (67). Taken together with our data, TAK1 plays a major role in both bone destruction and bone formation, albeit through different cytokine-mediated signaling networks.

Recently, two other groups reported mouse models for myeloid cell-specific deletion of TAK1 (27, 68) with emphasis on the role of TAK1 in response to LPS. Ajibade et al. (27) reported that specific deletion of TAK1 in the myeloid lineage resulted in mice with splenomegaly, lymphomegaly, and increased numbers of CD11b/Gr1 double positive cells in the bone marrow and spleen. Furthermore, LPS stimulation of TAK1-deficient neutrophils or peritoneal macrophages caused enhanced or similar activation of IKK, p38, and JNK compared to the corresponding control cells (27). In contrast, in their mouse model of myeloid cell-specific deletion of TAK1, Eftychi et al. (68) did not observe any gross morphological changes in the spleen and lymph nodes or differences in the myeloid cell population and showed that TAK1-deficient macrophages had impaired activation of NF-κB and JNK in response to LPS. These discrepancies could be due to the difference of the two TAK1-floxed mice used in these studies, one which has complete deletion of the TAK1 gene (27) while the other carries a truncated form of TAK1 (68). Nevertheless, the two groups reported similar results of hyperinflammatory responses following LPS challenge *in vitro* and *in vivo* (27, 68).

Furthermore, our study indicates that the deregulation of TAK1 expression leads to apoptosis and necroptosis, which raises the question of whether the cell inflammation and cell death observed in some conditional TAK1-deficient mice could be attenuated by the simultaneous deletion of caspase-8 and RIP3 genes (38, 39). These findings also indicate that the kinase activity status of TAK1 should be investigated in pathological tissue injury (e.g., renal or myocardial ischemia reperfusion injury).

In summary, we found that TAK1 promotes cell survival by blocking the TNF-α-induced cell death pathways of apoptosis and necroptosis and that TAK1 is an essential regulator of RANKL-induced osteoclastogenesis. Our study's findings thus add to our understanding of the multifaceted roles TAK1 plays in maintaining the balance between cell survival and cell death and regulating osteoclast development.

ACKNOWLEDGMENTS

This work was supported in part by institutional start-up funds from The University of Texas M. D. Anderson Cancer Center, an award from the Rolanette and Berdon Lawrence Bone Disease Program of Texas (to B.L.), the National Institutes of Health through a Research Project Grant (R01AR053540 to B.G.D.), and M. D. Anderson's Cancer Center Support Grant (CA016672).

REFERENCES

1. **Dougall WC, Glaccum M, Charrier K, Rohrbach K, Brasel K, De Smedt T, Daro E, Smith J, Tometsko ME, Maliszewski CR, Armstrong A, Shen V, Bain S, Cosman D, Anderson D, Morrissey PJ, Peschon JJ, Schuh J.** 1999. RANK is essential for osteoclast and lymph node development. Genes Dev. **13**:2412–2424.
2. **Kong YY, Yoshida H, Sarosi I, Tan HL, Timms E, Capparelli C, Morony S, Oliveira-dos Santos AJ, Van G, Itie A, Khoo W, Wakeham A, Dunstan CR, Lacey DL, Mak TW, Boyle WJ, Penninger JM.** 1999. OPGL is a key regulator of osteoclastogenesis, lymphocyte development and lymph-node organogenesis. Nature **397**:315–323.
3. **Darnay BG, Besse A, Poblenz AT, Lamothe B, Jacoby JJ.** 2007. TRAFs in RANK signaling. Adv. Exp. Med. Biol. **597**:152–159.
4. **Teitelbaum SL.** 2007. Osteoclasts: what do they do and how do they do it? Am. J. Pathol. **170**:427–435.
5. **Lomaga MA, Yeh WC, Sarosi I, Duncan GS, Furlonger C, Ho A, Morony S, Capparelli C, Van G, Kaufman S, van der Heiden A, Itie A, Wakeham A, Khoo W, Sasaki T, Cao Z, Penninger JM, Paige CJ, Lacey DL, Dunstan CR, Boyle WJ, Goeddel DV, Mak TW.** 1999. TRAF6 deficiency results in osteopetrosis and defective interleukin-1, CD40, and LPS signaling. Genes Dev. **13**:1015–1024.
6. **Naito A, Azuma S, Tanaka S, Miyazaki T, Takaki S, Takatsu K, Nakao K, Nakamura K, Katsuki M, Yamamoto T, Inoue J.** 1999. Severe osteopetrosis, defective interleukin-1 signalling and lymph node organogenesis in TRAF6-deficient mice. Genes Cells **4**:353–362.
7. **Lamothe B, Campos AD, Webster WK, Gopinathan A, Hur L, Darnay BG.** 2008. The RING domain and first zinc finger of TRAF6 coordinate signaling by interleukin-1, lipopolysaccharide, and RANKL. J. Biol. Chem. **283**:24871–24880.
8. **Lamothe B, Webster WK, Gopinathan A, Besse A, Campos AD, Darnay BG.** 2007. TRAF6 ubiquitin ligase is essential for RANKL signaling and osteoclast differentiation. Biochem. Biophys. Res. Commun. **359**:1044–1049.
9. **Otero JE, Dai S, Foglia D, Alhawagri M, Vacher J, Pasparakis M, Abu-Amer Y.** 2008. Defective osteoclastogenesis by IKKbeta-null precursors is a result of receptor activator of NF-kappaB ligand (RANKL)-induced JNK-dependent apoptosis and impaired differentiation. J. Biol. Chem. **283**:24546–24553.
10. **Ruocco MG, Maeda S, Park JM, Lawrence T, Hsu LC, Cao Y, Schett G, Wagner EF, Karin M.** 2005. I{kappa}B kinase (IKK){beta}, but not IKK{alpha}, is a critical mediator of osteoclast survival and is required for inflammation-induced bone loss. J. Exp. Med. **201**:1677–1687.
11. **Sato S, Sanjo H, Takeda K, Ninomiya-Tsuji J, Yamamoto M, Kawai T, Matsumoto K, Takeuchi O, Akira S.** 2005. Essential function for the kinase TAK1 in innate and adaptive immune responses. Nat. Immunol. **6**:1087–1095.
12. **Shim JH, Xiao C, Paschal AE, Bailey ST, Rao P, Hayden MS, Lee KY, Bussey C, Steckel M, Tanaka N, Yamada G, Akira S, Matsumoto K, Ghosh S.** 2005. TAK1, but not TAB1 or TAB2, plays an essential role in multiple signaling pathways in vivo. Genes Dev. **19**:2668–2681.
13. **Deng L, Wang C, Spencer E, Yang L, Braun A, You J, Slaughter C, Pickart C, Chen ZJ.** 2000. Activation of the IkappaB kinase complex by TRAF6 requires a dimeric ubiquitin-conjugating enzyme complex and a unique polyubiquitin chain. Cell **103**:351–361.
14. **Lamothe B, Besse A, Campos AD, Webster WK, Wu H, Darnay BG.** 2007. Site-specific Lys-63-linked tumor necrosis factor receptor-associated Factor 6 auto-ubiquitination is a critical determinant of IkappaB kinase activation. J. Biol. Chem. **282**:4102–4112.
15. **Wang C, Deng L, Hong M, Akkaraju GR, Inoue J, Chen ZJ.** 2001. TAK1 is a ubiquitin-dependent kinase of MKK and IKK. Nature **412**:346–351.
16. **Yin Q, Lin SC, Lamothe B, Lu M, Lo YC, Hura G, Zheng L, Rich RL, Campos AD, Myszka DG, Lenardo MJ, Darnay BG, Wu H.** 2009. E2 interaction and dimerization in the crystal structure of TRAF6. Nat. Struct. Mol. Biol. **16**:658–666.
17. **Huang H, Ryu J, Ha J, Chang EJ, Kim HJ, Kim HM, Kitamura T, Lee ZH, Kim HH.** 2006. Osteoclast differentiation requires TAK1 and MKK6 for NFATc1 induction and NF-kappaB transactivation by RANKL. Cell Death Differ. **13**:1879–1891.
18. **Lee SW, Han SI, Kim HH, Lee ZH.** 2002. TAK1-dependent activation of AP-1 and c-Jun N-terminal kinase by receptor activator of NF-kappaB. J. Biochem. Mol. Biol. **35**:371–376.
19. **Mizukami J, Takaesu G, Akatsuka H, Sakurai H, Ninomiya-Tsuji J, Matsumoto K, Sakurai N.** 2002. Receptor activator of NF-kappaB ligand (RANKL) activates TAK1 mitogen-activated protein kinase kinase kinase through a signaling complex containing RANK, TAB2, and TRAF6. Mol. Cell. Biol. **22**:992–1000.
20. **Besse A, Lamothe B, Campos AD, Webster WK, Maddineni U, Lin SC, Wu H, Darnay BG.** 2007. TAK1-dependent signaling requires functional interaction with TAB2/TAB3. J. Biol. Chem. **282**:3918–3928.
21. **Clausen BE, Burkhardt C, Reith W, Renkawitz R, Forster I.** 1999. Conditional gene targeting in macrophages and granulocytes using LysMcre mice. Transgenic Res. **8**:265–277.
22. **Nakamura T, Imai Y, Matsumoto T, Sato S, Takeuchi K, Igarashi K, Harada Y, Azuma Y, Krust A, Yamamoto Y, Nishina H, Takeda S, Takayanagi H, Metzger D, Kanno J, Takaoka K, Martin TJ, Chambon P, Kato S.** 2007. Estrogen prevents bone loss via estrogen receptor alpha and induction of Fas ligand in osteoclasts. Cell **130**:811–823.
23. **Xie M, Zhang D, Dyck JR, Li Y, Zhang H, Morishima M, Mann DL, Taffet GE, Baldini A, Khoury DS, Schneider MD.** 2006. A pivotal role for endogenous TGF-beta-activated kinase-1 in the LKB1/AMP-activated protein kinase energy-sensor pathway. Proc. Natl. Acad. Sci. U. S. A. **103**:17378–17383.
24. **Poblenz AT, Jacoby JJ, Singh S, Darnay BG.** 2007. Inhibition of RANKL-mediated osteoclast differentiation by selective TRAF6 decoy peptides. Biochem. Biophys. Res. Commun. **359**:510–515.
25. **Parfitt AM, Drezner MK, Glorieux FH, Kanis JA, Malluche H, Meunier PJ, Ott SM, Recker RR.** 1987. Bone histomorphometry: standardization of nomenclature, symbols, and units. Report of the ASBMR Histomorphometry Nomenclature Committee. J. Bone Miner. Res. **2**:595–610.
26. **Micheau O, Tschopp J.** 2003. Induction of TNF receptor I-mediated apoptosis via two sequential signaling complexes. Cell **114**:181–190.
27. **Ajibade AA, Wang Q, Cui J, Zou J, Xia X, Wang M, Tong Y, Hui W, Liu D, Su B, Wang HY, Wang RF.** 2012. TAK1 negatively regulates NF-kappaB and p38 MAP kinase activation in Gr-1+CD11b+ neutrophils. Immunity **36**:43–54.
28. **Omori E, Matsumoto K, Sanjo H, Sato S, Akira S, Smart RC, Ninomiya-Tsuji J.** 2006. TAK1 is a master regulator of epidermal homeostasis involving skin inflammation and apoptosis. J. Biol. Chem. **281**:19610–19617.
29. **Omori E, Morioka S, Matsumoto K, Ninomiya-Tsuji J.** 2008. TAK1 regulates reactive oxygen species and cell death in keratinocytes, which is essential for skin integrity. J. Biol. Chem. **283**:26161–26168.
30. **Sato S, Sanjo H, Tsujimura T, Ninomiya-Tsuji J, Yamamoto M, Kawai T, Takeuchi O, Akira S.** 2006. TAK1 is indispensable for development of T cells and prevention of colitis by the generation of regulatory T cells. Int. Immunol. **18**:1405–1411.
31. **Wan YY, Chi H, Xie M, Schneider MD, Flavell RA.** 2006. The kinase TAK1 integrates antigen and cytokine receptor signaling for T cell development, survival and function. Nat. Immunol. **7**:851–858.
32. **Fleetwood AJ, Lawrence T, Hamilton JA, Cook AD.** 2007. Granulocyte-macrophage colony-stimulating factor (CSF) and macrophage CSF-dependent macrophage phenotypes display differences in cytokine profiles and transcription factor activities: implications for CSF blockade in inflammation. J. Immunol. **178**:5245–5252.
33. **Kroemer G, Galluzzi L, Vandenabeele P, Abrams J, Alnemri ES, Baehrecke EH, Blagosklonny MV, El-Deiry WS, Golstein P, Green DR, Hengartner M, Knight RA, Kumar S, Lipton SA, Malorni W, Nunez G,**

Peter ME, Tschopp J, Yuan J, Piacentini M, Zhivotovsky B, Melino G. 2009. Classification of cell death: recommendations of the Nomenclature Committee on Cell Death 2009. Cell Death Differ. **16**:3–11.
34. **Vandenabeele P, Galluzzi L, Vanden Berghe T, Kroemer G.** 2010. Molecular mechanisms of necroptosis: an ordered cellular explosion. Nat. Rev. Mol. Cell Biol. **11**:700–714.
35. **Degterev A, Hitomi J, Germscheid M, Ch'en IL, Korkina O, Teng X, Abbott D, Cuny GD, Yuan C, Wagner G, Hedrick SM, Gerber SA, Lugovskoy A, Yuan J.** 2008. Identification of RIP1 kinase as a specific cellular target of necrostatins. Nat. Chem. Biol. **4**:313–321.
36. **Vandenabeele P, Declercq W, Van Herreweghe F, Vanden Berghe T.** 2010. The role of the kinases RIP1 and RIP3 in TNF-induced necrosis. Sci. Signal. **3**:re4. doi:10.1126/scisignal.3115re4.
37. **Fan Y, Yu Y, Shi Y, Sun W, Xie M, Ge N, Mao R, Chang A, Xu G, Schneider MD, Zhang H, Fu S, Qin J, Yang J.** 2010. Lysine 63-linked polyubiquitination of TAK1 at lysine 158 is required for tumor necrosis factor alpha- and interleukin-1beta-induced IKK/NF-kappaB and JNK/AP-1 activation. J. Biol. Chem. **285**:5347–5360.
38. **Kaiser WJ, Upton JW, Long AB, Livingston-Rosanoff D, Daley-Bauer LP, Hakem R, Caspary T, Mocarski ES.** 2011. RIP3 mediates the embryonic lethality of caspase-8-deficient mice. Nature **471**:368–372.
39. **Oberst A, Dillon CP, Weinlich R, McCormick LL, Fitzgerald P, Pop C, Hakem R, Salvesen GS, Green DR.** 2011. Catalytic activity of the caspase-8-FLIP(L) complex inhibits RIPK3-dependent necrosis. Nature **471**:363–367.
40. **Upton JW, Kaiser WJ, Mocarski ES.** 2010. Virus inhibition of RIP3-dependent necrosis. Cell Host Microbe **7**:302–313.
41. **Ito Y, Teitelbaum SL, Zou W, Zheng Y, Johnson JF, Chappel J, Ross FP, Zhao H.** 2010. Cdc42 regulates bone modeling and remodeling in mice by modulating RANKL/M-CSF signaling and osteoclast polarization. J. Clin. Invest. **120**:1981–1993.
42. **Iwasawa M, Miyazaki T, Nagase Y, Akiyama T, Kadono Y, Nakamura M, Oshima Y, Yasui T, Matsumoto T, Nakamura T, Kato S, Hennighausen L, Nakamura K, Tanaka S.** 2009. The antiapoptotic protein Bcl-xL negatively regulates the bone-resorbing activity of osteoclasts in mice. J. Clin. Invest. **119**:3149–3159.
43. **Yang C, McCoy K, Davis JL, Schmidt-Supprian M, Sasaki Y, Faccio R, Novack DV.** 2010. NIK stabilization in osteoclasts results in osteoporosis and enhanced inflammatory osteolysis. PLoS One **5**:e15383. doi:10.1371/journal.pone.0015383.
44. **Mizoguchi F, Izu Y, Hayata T, Hemmi H, Nakashima K, Nakamura T, Kato S, Miyasaka N, Ezura Y, Noda M.** 2010. Osteoclast-specific Dicer gene deficiency suppresses osteoclastic bone resorption. J. Cell. Biochem. **109**:866–875.
45. **Miyauchi Y, Ninomiya K, Miyamoto H, Sakamoto A, Iwasaki R, Hoshi H, Miyamoto K, Hao W, Yoshida S, Morioka H, Chiba K, Kato S, Tokuhisa T, Saitou M, Toyama Y, Suda T, Miyamoto T.** 2010. The Blimp1-Bcl6 axis is critical to regulate osteoclast differentiation and bone homeostasis. J. Exp. Med. **207**:751–762.
46. **Croke M, Ross FP, Korhonen M, Williams DA, Zou W, Teitelbaum SL.** 2011. Rac deletion in osteoclasts causes severe osteopetrosis. J. Cell Sci. **124**:3811–3821.
47. **Liu HH, Xie M, Schneider MD, Chen ZJ.** 2006. Essential role of TAK1 in thymocyte development and activation. Proc. Natl. Acad. Sci. U. S. A. **103**:11677–11682.
48. **O'Donnell MA, Legarda-Addison D, Skountzos P, Yeh WC, Ting AT.** 2007. Ubiquitination of RIP1 regulates an NF-kappaB-independent cell-death switch in TNF signaling. Curr. Biol. **17**:418–424.
49. **McComb S, Cheung HH, Korneluk RG, Wang S, Krishnan L, Sad S.** 2012. cIAP1 and cIAP2 limit macrophage necroptosis by inhibiting Rip1 and Rip3 activation. Cell Death Differ. **19**:1791–1801.
50. **Wu YT, Tan HL, Huang Q, Sun XJ, Zhu X, Shen HM.** 2011. zVAD-induced necroptosis in L929 cells depends on autocrine production of TNFalpha mediated by the PKC-MAPKs-AP-1 pathway. Cell Death Differ. **18**:26–37.
51. **Christofferson DE, Li Y, Hitomi J, Zhou W, Upperman C, Zhu H, Gerber SA, Gygi S, Yuan J.** 2012. A novel role for RIP1 kinase in mediating TNFalpha production. Cell Death Dis. **3**:e320. doi:10.1038/cddis.2012.64.
52. **Hitomi J, Christofferson DE, Ng A, Yao J, Degterev A, Xavier RJ, Yuan J.** 2008. Identification of a molecular signaling network that regulates a cellular necrotic cell death pathway. Cell **135**:1311–1323.
53. **Arslan SC, Scheidereit C.** 2011. The prevalence of TNFalpha-induced necrosis over apoptosis is determined by TAK1-RIP1 interplay. PLoS One **6**:e26069. doi:10.1371/journal.pone.0026069.
54. **Wang L, Du F, Wang X.** 2008. TNF-alpha induces two distinct caspase-8 activation pathways. Cell **133**:693–703.
55. **Vanlangenakker N, Vanden Berghe T, Bogaert P, Laukens B, Zobel K, Deshayes K, Vucic D, Fulda S, Vandenabeele P, Bertrand MJ.** 2011. cIAP1 and TAK1 protect cells from TNF-induced necrosis by preventing RIP1/RIP3-dependent reactive oxygen species production. Cell Death Differ. **18**:656–665.
56. **Cho YS, Challa S, Moquin D, Genga R, Ray TD, Guildford M, Chan FK.** 2009. Phosphorylation-driven assembly of the RIP1-RIP3 complex regulates programmed necrosis and virus-induced inflammation. Cell **137**:1112–1123.
57. **Schuman J, Chen Y, Podd A, Yu M, Liu HH, Wen R, Chen ZJ, Wang D.** 2009. A critical role of TAK1 in B-cell receptor-mediated nuclear factor kappaB activation. Blood **113**:4566–4574.
58. **Mellis DJ, Itzstein C, Helfrich MH, Crockett JC.** 2011. The skeleton: a multi-functional complex organ: the role of key signalling pathways in osteoclast differentiation and in bone resorption. J. Endocrinol. **211**:131–143.
59. **David JP, Sabapathy K, Hoffmann O, Idarraga MH, Wagner EF.** 2002. JNK1 modulates osteoclastogenesis through both c-Jun phosphorylation-dependent and -independent mechanisms. J. Cell Sci. **115**:4317–4325.
60. **Li X, Udagawa N, Itoh K, Suda K, Murase Y, Nishihara T, Suda T, Takahashi N.** 2002. p38 MAPK-mediated signals are required for inducing osteoclast differentiation but not for osteoclast function. Endocrinology **143**:3105–3113.
61. **Matsumoto M, Sudo T, Saito T, Osada H, Tsujimoto M.** 2000. Involvement of p38 mitogen-activated protein kinase signaling pathway in osteoclastogenesis mediated by receptor activator of NF-kappa B ligand (RANKL). J. Biol. Chem. **275**:31155–31161.
62. **Sayama K, Hanakawa Y, Nagai H, Shirakata Y, Dai X, Hirakawa S, Tokumaru S, Tohyama M, Yang L, Sato S, Shizuo A, Hashimoto K.** 2006. Transforming growth factor-beta-activated kinase 1 is essential for differentiation and the prevention of apoptosis in epidermis. J. Biol. Chem. **281**:22013–22020.
63. **Buhling F, Rocken C, Brasch F, Hartig R, Yasuda Y, Saftig P, Bromme D, Welte T.** 2004. Pivotal role of cathepsin K in lung fibrosis. Am. J. Pathol. **164**:2203–2216.
64. **Quintanilla-Dieck MJ, Codriansky K, Keady M, Bhawan J, Runger TM.** 2009. Expression and regulation of cathepsin K in skin fibroblasts. Exp. Dermatol. **18**:596–602.
65. **Runger TM, Quintanilla-Dieck MJ, Bhawan J.** 2007. Role of cathepsin K in the turnover of the dermal extracellular matrix during scar formation. J. Invest. Dermatol. **127**:293–297.
66. **Boonen S, Rosenberg E, Claessens F, Vanderschueren D, Papapoulos S.** 2012. Inhibition of cathepsin K for treatment of osteoporosis. Curr. Osteoporos. Rep. **10**:73–79.
67. **Greenblatt MB, Shim JH, Zou W, Sitara D, Schweitzer M, Hu D, Lotinun S, Sano Y, Baron R, Park JM, Arthur S, Xie M, Schneider MD, Zhai B, Gygi S, Davis R, Glimcher LH.** 2010. The p38 MAPK pathway is essential for skeletogenesis and bone homeostasis in mice. J. Clin. Invest. **120**:2457–2473.
68. **Eftychi C, Karagianni N, Alexiou M, Apostolaki M, Kollias G.** 2012. Myeloid TAKL acts as a negative regulator of the LPS response and mediates resistance to endotoxemia. PLoS One **7**:e31550. doi:10.1371/journal.pone.0031550.